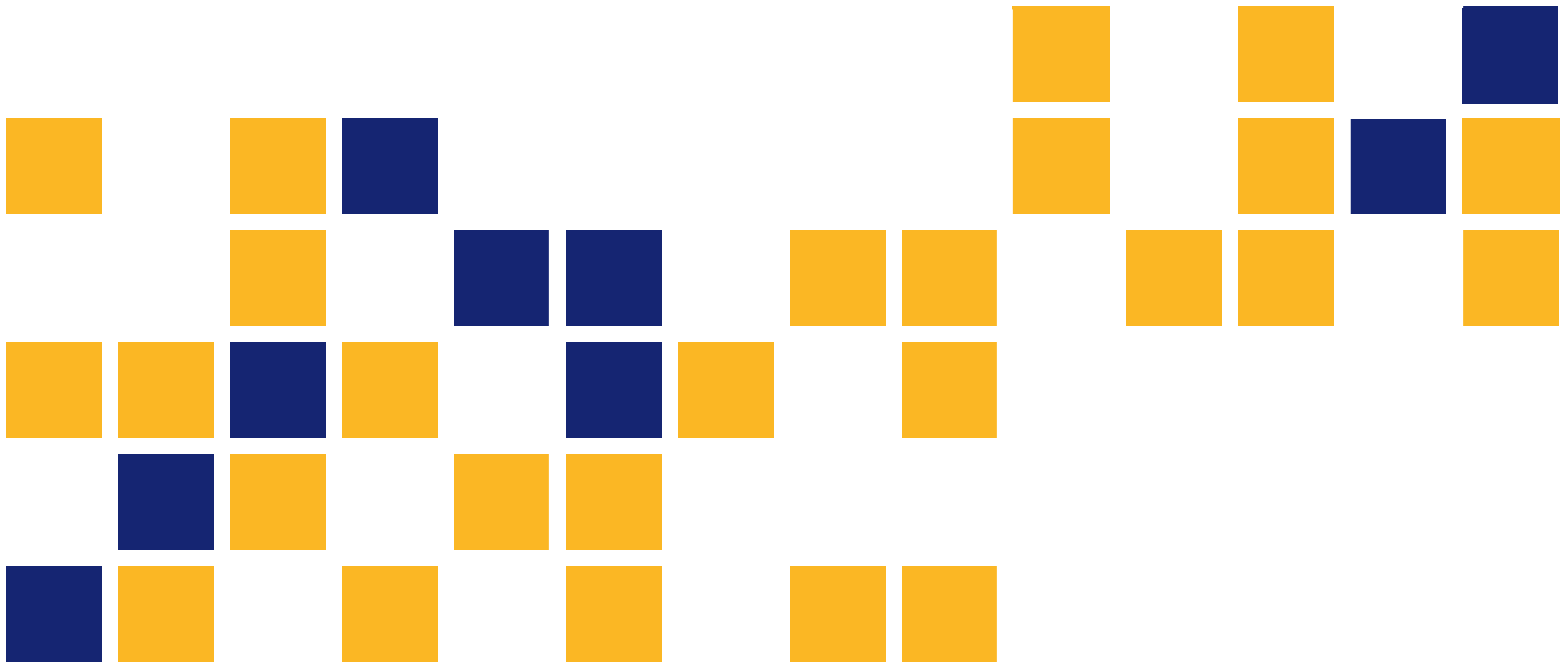# Tolerable Strains for Hot Mix Asphalt Overlays over Concrete Pavements

Jie Han, Ph.D., P.E.
Ashwani Gautam, M.S.
Sanat K. Pokharel, Ph.D.
Robert L. Parsons, Ph.D., P.E.

The University of Kansas

AD ASTRA PER ASPERA

Kansas
Department of Transportation

This page intentionally left blank.

1	Report No. K-TRAN: KU-08-3	2	Government Accession No.	3	Recipient Catalog No.
4	**Title and Subtitle** Tolerable Strains for Hot Mix Asphalt Overlays over Concrete Pavements			**5**	**Report Date** January 2013
				6	**Performing Organization Code**
7	**Author(s)** Jie Han, Ph.D., P.E.; Ashwani Gautam, M.S.; Sanat K. Pokharel, Ph.D.; Robert L. Parsons, Ph.D., P.E.			**8**	**Performing Organization Report No.**
9	**Performing Organization Name and Address** University of Kansas Civil, Environmental & Architectural Engineering Department 1530 West 15th Street Lawrence, Kansas 66045-7609			**10**	**Work Unit No. (TRAIS)**
				11	**Contract or Grant No.** C1727
12	**Sponsoring Agency Name and Address** Kansas Department of Transportation Bureau of Materials and Research 700 SW Harrison Street Topeka, Kansas 66603-3745			**13**	**Type of Report and Period Covered** Final Report August 2007–June 2012
				14	**Sponsoring Agency Code** RE-0470-01
15	**Supplementary Notes**				

16 Abstract

Due to change of temperature and/or moisture, freezing-thaw cycles, loss of subgrade support by erosion, and traffic loading, concrete pavements can develop different types of distresses during service life. Hot mix asphalt (HMA) overlays are commonly used to improve the serviceability of damaged concrete pavements. The most challenging issue for HMA overlays over concrete pavements is the development of reflection cracks through the overlays at the locations of joints and existing cracks on concrete pavements. Even though different techniques have been used to overcome this issue, they often do not yield satisfactory results and performance. Cracking of HMA overlays results from intolerable tensile strain and/or shear movement developed in the overlays due to the movement of concrete pavements. Limited studies have been conducted so far to determine the tolerable tensile strain and shear deformation of HMA overlays on concrete pavements. If the strain and shear deformation the HMA can endure are known, the methods that will limit or prevent that strain and deformation can be sought. This research experimentally determined the tolerable tensile strain and the relative shear movement of the HMA overlays. Direct shear tests and semi-circular bend tests of HMA specimens and HMA overlay loading tests under static and cyclic loading on gapped concrete blocks were conducted in this research.

HMA materials from two Kansas Department of Transportation (KDOT) projects, namely 089 C-4318-01 (Mix 1) and 56-29 KA-1087-01 (Mix 2), were used in the laboratory study. All testing was conducted at room temperature. Considering typical HMA overlay thicknesses used in Kansas, the selected thicknesses of the HMA overlays were 1.5 and 2.0 inches. Direct shear tests and semi-circular bend tests were conducted on these chosen HMA mixtures to characterize their shear and tensile properties respectively. Overlay loading tests were conducted on HMA overlays adhered to gapped concrete blocks to evaluate the interaction between the HMA overlays and the concrete blocks with a gap subjected to static or cyclic loading. Steel bars having a diameter of 0.25, 0.375, or 0.5 inches were used as spacers to create a gap in a direct shear test in the lab. These gaps simulate joints in concrete pavements. Measured relative shear displacements of these HMA specimens at failure varied from 6.0 % to 9.0 % of the specimen thickness depending upon the simulated gap width. Tolerable tensile strains of Mix 1 specimens under fatigue loading in the semi-circular bend tests were from 1.2% to 4% while those of Mix 2 specimens were from 0.6% to 1.4%. Test results show that the compressive load capacity of a specimen under the semi-circular bend test was linearly correlated to the shear load capacity of the specimen at the same mix and thickness under the direct shear test. Specimens at the onset of cracking in the overlay loading tests had the permanent vertical displacements with similar magnitudes as the shear displacements corresponding to the shear load capacities in the direct shear tests. The tolerable tensile strains of HMA specimens in the overlay tests were smaller than those in the semi-circular bend tests; however, an increase of the applied load or gap width minimized their differences. The overlay loading tests showed that the cracking could be avoided if the tensile strains in the HMA overlays were less than 0.5%.

Based on the HMA mixes, the specimen thicknesses, the gaps between the concrete blocks, the load levels, and the test temperatures used in this research, it can be concluded that: (1) the shear failure could be avoided if the shear deformation of the HMA overlay was less than 6% of the overlay thickness and (2) the cracking could be avoided if the tensile strain in the HMA overlay was less than 0.6%. The methods that will limit or prevent reflection cracks due to shear deformation and tensile strain should be sought in a future study.

17	**Key Words** HMA, Hot Mix Asphalt, Portland Cement Concrete Pavement, Reflection Cracks	**18**	**Distribution Statement** No restrictions. This document is available to the public through the National Technical Information Service www.ntis.gov.		
19	**Security Classification (of this report)** Unclassified	**20**	**Security Classification (of this page)** Unclassified	**21 No. of pages** 113	**22 Price**

Form DOT F 1700.7 (8-72)

Tolerable Strains for Hot Mix Asphalt Overlays over Concrete Pavements

Final Report

Prepared by

Jie Han, Ph.D., P.E.
Ashwani Gautam, M.S.
Sanat K. Pokharel, Ph.D.
Robert L. Parsons, Ph.D., P.E.
The University of Kansas

PREFACE

The Kansas Department of Transportation's (KDOT) Kansas Transportation Research and New-Developments (K-TRAN) Research Program funded this research project. It is an ongoing, cooperative and comprehensive research program addressing transportation needs of the state of Kansas utilizing academic and research resources from KDOT, Kansas State University and the University of Kansas. Transportation professionals in KDOT and the universities jointly develop the projects included in the research program.

NOTICE

The authors and the state of Kansas do not endorse products or manufacturers. Trade and manufacturers names appear herein solely because they are considered essential to the object of this report.

This information is available in alternative accessible formats. To obtain an alternative format, contact the Office of Transportation Information, Kansas Department of Transportation, 700 SW Harrison, Topeka, Kansas 66603-3754 or phone (785) 296-3585 (Voice) (TDD).

DISCLAIMER

The contents of this report reflect the views of the authors who are responsible for the facts and accuracy of the data presented herein. The contents do not necessarily reflect the views or the policies of the state of Kansas. This report does not constitute a standard, specification or regulation.

Abstract

Due to change of temperature and/or moisture, freezing-thaw cycles, loss of subgrade support by erosion, and traffic loading, concrete pavements can develop different types of distresses during service life. Hot mix asphalt (HMA) overlays are commonly used to improve the serviceability of damaged concrete pavements. The most challenging issue for HMA overlays over concrete pavements is the development of reflection cracks through the overlays at the locations of joints and existing cracks on concrete pavements. Even though different techniques have been used to overcome this issue, they often do not yield satisfactory results and performance. Cracking of HMA overlays results from intolerable tensile strain and/or shear movement developed in the overlays due to the movement of concrete pavements. Limited studies have been conducted so far to determine the tolerable tensile strain and shear deformation of HMA overlays on concrete pavements. If the strain and shear deformation the HMA can endure are known, the methods that will limit or prevent that strain and deformation can be sought. This research experimentally determined the tolerable tensile strain and the relative shear movement of the HMA overlays. Direct shear tests and semi-circular bend tests of HMA specimens and HMA overlay loading tests under static and cyclic loading on gapped concrete blocks were conducted in this research.

HMA materials from two Kansas Department of Transportation (KDOT) projects, namely 089 C-4318-01 (Mix 1) and 56-29 KA-1087-01 (Mix 2), were used in the laboratory study. All testing was conducted at room temperature. Considering typical HMA overlay thicknesses used in Kansas, the selected thicknesses of the HMA overlays were 1.5 and 2.0 inches. Direct shear tests and semi-circular bend tests were conducted on these chosen HMA mixtures to characterize their shear and tensile properties respectively. Overlay loading tests were conducted on HMA overlays adhered to gapped concrete blocks to evaluate the interaction between the HMA overlays and the concrete blocks with a gap subjected to static or cyclic loading. Steel bars having a diameter of 0.25, 0.375, or 0.5 inches were used as spacers to create a gap in a direct shear test in the lab. These gaps simulate joints in concrete pavements. Measured relative shear displacements of these HMA specimens at failure varied from 6.0 % to 9.0 % of the specimen thickness depending upon the simulated gap width. Tolerable tensile strains of Mix 1 specimens

under fatigue loading in the semi-circular bend tests were from 1.2% to 4% while those of Mix 2 specimens were from 0.6% to 1.4%. Test results show that the compressive load capacity of a specimen under the semi-circular bend test was linearly correlated to the shear load capacity of the specimen at the same mix and thickness under the direct shear test. Specimens at the onset of cracking in the overlay loading tests had the permanent vertical displacements with similar magnitudes as the shear displacements corresponding to the shear load capacities in the direct shear tests. The tolerable tensile strains of HMA specimens in the overlay tests were smaller than those in the semi-circular bend tests; however, an increase of the applied load or gap width minimized their differences. The overlay loading tests showed that the cracking could be avoided if the tensile strains in the HMA overlays were less than 0.5%.

Based on the HMA mixes, the specimen thicknesses, the gaps between the concrete blocks, the load levels, and the test temperatures used in this research, it can be concluded that: (1) the shear failure could be avoided if the shear deformation of the HMA overlay was less than 6% of the overlay thickness and (2) the cracking could be avoided if the tensile strain in the HMA overlay was less than 0.6%. The methods that will limit or prevent reflection cracks due to shear deformation and tensile strain should be sought in a future study.

Acknowledgements

Table of Contents

List of Tables

List of Figures

Chapter 1: Introduction

1.1 Background

Due to temperature and/or moisture changes, freezing-thaw cycles, loss of subgrade support by erosion, and traffic loading, concrete pavements can develop different types of distresses during service life. Hot Mix Asphalt (HMA) overlays are commonly used to improve the serviceability of damaged concrete pavements. Some HMA overlays prematurely exhibit a cracking pattern similar to what existed in the old, underlying concrete pavement. The cracking in the overlays is often due to inability of the HMA overlays to endure tensile and shear strains. Tensile and shear strains develop because of movement of jointed or cracked slabs of underlying old pavements concentrated around pre-existing cracks. This movement is caused by a combination of traffic loading (differential deflections at cracks) and expansion and contraction of existing pavements due to change in temperature and/or moisture. Such movements induce shear and tensile strains in the HMA overlay. When the induced tensile and shear stresses corresponding to the strains become higher than tensile and shear strengths of HMA, cracks develop in the overlay and propagate with the cycles of movement. The phenomenon of propagation of existing cracks from old pavements to HMA overlays is called *reflection cracking*.

1.2 Problem Statement

The most challenging issue for HMA overlays over concrete pavements is the development of reflection cracks through the overlays at the locations of joints and existing cracks on concrete pavements. Even though different techniques have been used to overcome this issue, they often do not yield satisfactory results and performance. Cracking of HMA overlays results from intolerable tensile and/or shear strains developed in overlays due to the movement of concrete pavements. Past research has focused on tensile strengths, rutting, and fatigue behavior of HMA; however, very limited studies have been conducted to determine tolerable tensile strain and relative shear movement of HMA overlays on concrete pavements. If the strain and the shear deformation the HMA can endure are known, methods that limit or prevent that strain and shear deformation can be sought.

1

1.3 Objective

The main objective of this study was to experimentally determine the tolerable tensile strain and relative shear deformation/strength in HMA overlays under cyclic tensile stresses and monotonic shear stresses. Results from this research can be used to design HMA overlays and develop mitigation methods to minimize possible failure of HMA overlays on concrete pavements.

Direct shear box, semi-circular bend, and overlay loading tests were conducted on selected mixes from the Kansas Department of Transportation (KDOT) to determine the tolerable shear deformation/strength and tensile strain of HMA overlays. Tolerable shear strength is defined as the maximum shear force the specimen can carry. Tolerable relative shear deformation is defined as the movement corresponding to the maximum shear force divided by the thickness of the HMA overlay. Tolerable tensile strength is defined as the tensile strength of the HMA overlay when a crack starts to appear. The tolerable tensile strain is the strain corresponding to the tolerable tensile strength. Direct shear box tests can give the maximum shear force HMA can endure before failure. Static and cyclic semi-circular bend tests can be used to determine the tensile strength and strain of the HMA overlay. The static and cyclic overlay loading tests can evaluate the performance of HMA overlays on gapped concrete blocks on deformable subgrade.

1.4 Organization

This report contains five chapters:

Chapter 1 presents the background, the problem statement, the objective of the research, and the organization of this research report.

Chapter 2 provides a literature review of the mechanisms of reflection cracking in HMA overlays, the state of the research to evaluate the HMA overlays, and the techniques to minimize reflection cracks.

Chapter 3 documents the experimental study carried on for the present research, which includes the use of the equipment, the material characterization, the preparation of the samples, and the test procedures.

Chapter 4 presents the test results obtained from the experimental study of direct shear box, semi-circular bend, and overlay loading tests for HMA specimens.

Chapter 5 summarizes the test results and makes conclusions and recommendations based on this research.

Chapter 2: Literature Review

2.1 Introduction

Using Hot Mix Asphalt (HMA) for rehabilitation of aged and jointed concrete pavements or asphalt pavements is problematic and susceptible to reflection cracking. Reflection cracking is one of the most important factors causing premature failure of HMA overlays and hence the pavements. Reflection cracking has been studied for a long time, but it still occurs and costs millions of dollars per year. Reflection cracking is generally defined as propagation of an existing crack or joint pattern from existing pavements to new HMA overlays. Occurrence of reflection cracks has caused significant maintenance and serviceability issues.

Many studies (for example, Abd El-Naby et al. 2002; Kim et al. 2003; Lee et al. 2007) have been undertaken to understand and prevent reflection cracking. Currently various methods exist to minimize reflection cracking but they often do not yield satisfactory results. Study of reflection cracking has been approached from different angles including numerical modeling, mechanistic modeling, field studies, and laboratory studies.

Reflection cracking occurs in HMA overlays because of their inability to withstand tensile and shear stresses created by vertical and horizontal movements of cracked or jointed pavements underneath. This research experimentally determined the maximum shear and tensile strengths and strains HMA overlays can withstand. When tolerable tensile and shear and tensile strengths and strains of HMA are known, methods can be sought to minimize or prevent the reflection cracking.

2.2 Mechanisms of Reflection Cracking

The basic mechanisms that are normally assumed to cause reflection cracking are vertical and horizontal movements of the pavement. The vertical movement of the pavement is mainly caused by moving traffic. The vertical movement in the HMA overlay is generally induced by differential movements of the underlying pavement. The horizontal movement of cracks and joints is caused by temperature and/or moisture changes. The vertical movement in the overlay induces a shear stress in the HMA. The horizontal movement of cracked or jointed slabs causes high tensile stresses and strains at the bottom of the asphalt overlay and results in reflection

4

cracking. This happens because at low temperature, asphalt concrete is stiff, brittle and it can not withstand large temperature-induced stresses. In addition to temperature changes in underlying cracked slabs, the total movement of the cracked slab is attributed to moisture changes, slab length, and stiffness properties of the overlaying material (Sherman et al. 1982).

Lee et al. (2007) illustrated different stages in the development of reflection cracking in HMA overlays over a cracked concrete pavement as shown in Figure 2.1. This process can be described in two modes. In Mode 1, the progress of reflection cracking is caused by horizontal movement of concrete slabs due to the change in temperature and/or moisture. In Mode 2, the vertical load from traffic causes the differential vertical movement of cracked concrete slabs and induces a large shear stress, and hence leads to shear failure.
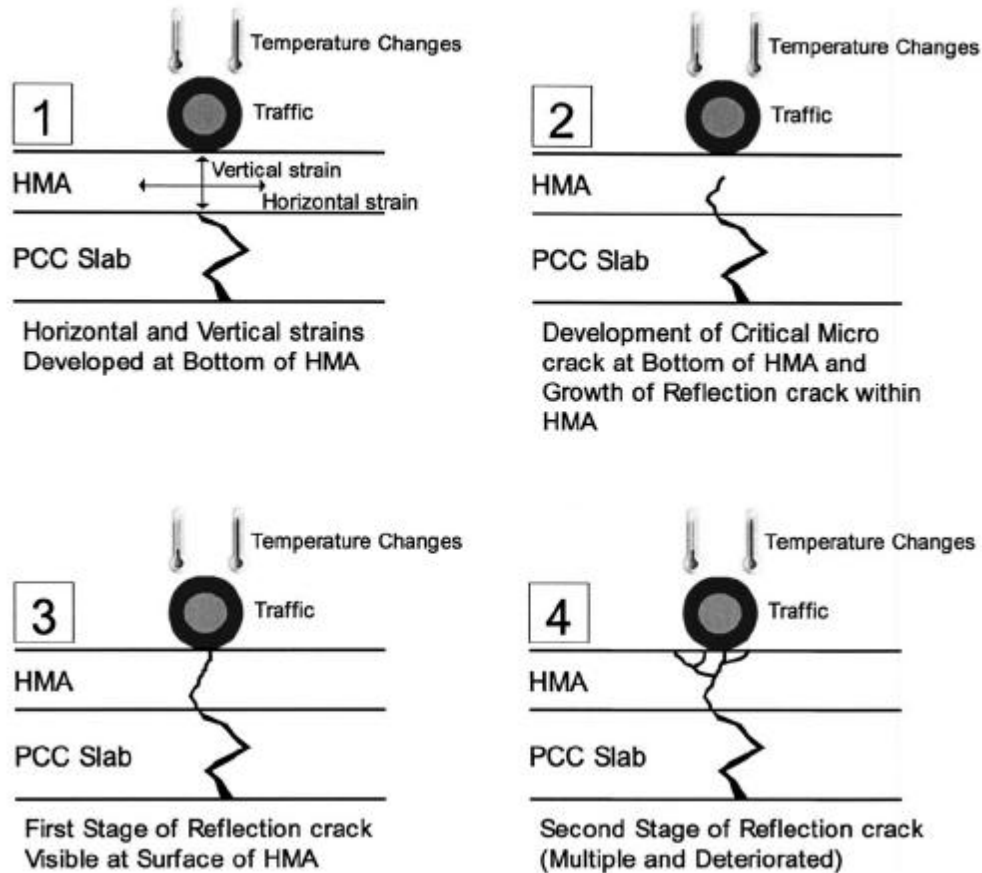
(Lee et al. 2007)

FIGURE 2.1
Different Stages in Development of Reflection Cracking on HMA Overlays

In another attempt to understand the process of reflection cracking, Francken et al. (1997) described different factors contributing to the development of reflection cracking. Traffic load can produce two types of movement in the cracked concrete slab that generate shear stresses (Figure 2.2a and c) due to relative vertical movement of cracked slabs and flexural stresses (Figure 2.2b) in the HMA overlay. In addition, due to temperature and/or moisture changes, the cracked concrete slab contracts and expands, inducing large tensile stress at the bottom of HMA overlay and causing progressive opening-up of joints and cracks (Figure 2.2d).
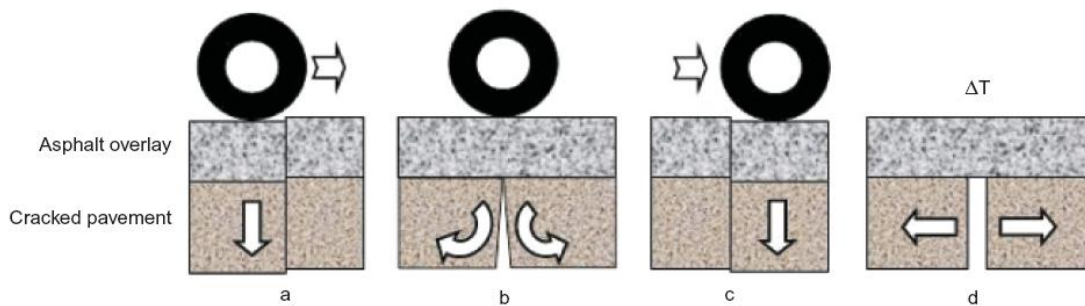
(Francken et al. 1997)

FIGURE 2.2
Movements in Pavement Joints and Cracks

2.3 Methods to Prevent Reflection Cracking

Literature review shows many attempts have been made to minimize reflection cracking. These methods include installation of a transition layer made of wire mesh, steel reinforcement, and sawing and sealing at the joint, etc. Using special materials as an overlay has also been explored. Rubber asphalt, fiber-reinforced asphalt, and polymer asphalt are other commonly explored options to prevent reflection cracking. Increasing thickness of the overlay has been adopted to minimize reflection cracking. These methods have partially helped to minimize the initiation and propagation of reflection cracks (Huffman et al. 1978; National Asphalt Pavement Association 1999).

In order to delay reflection cracking, several interlayer systems have been recently introduced. These interlayer systems may delay reflection cracking by two mechanisms: (1) reflection cracking can be retarded by using reinforcement systems, which are stiffer than

surrounded materials, such as geosynthetics or steel reinforcement and (2) a low modulus material is used to create a stress absorption layer.

The methods which have been used so far can be summarized as follows:

1. Use of geosynthetic or geogrid as reinforcement. (for example, Ellis et al. 2002)
2. Use of steel as reinforcement.
3. Crack and seat treatment on the existing concrete.
4. Stress absorbing membrane as an interlayer between overlay and concrete.
5. Using modified asphalt for overlay.
6. Using large thickness of asphalt overlay.
7. Use of a porous friction course to retard reflection cracks in asphalt overlay.
8. Rubblization of concrete (for example, Lee et al. 2007)

Button and Lytton (2006) provided guidelines for using geosynthetics to reduce reflection cracking in HMA overlays. They addressed the following issues: (a) when to consider geosynthetic products as an option, (b) cost considerations, (c) selection and storage of geosynthetics, (d) pavement design with geosynthetics, (e) construction inspection, (f) overlay construction with geosynthetics, and (g) potential construction problems. Button and Lytton (2006) proposed three scenarios of cracking and described when the use of geosynthetics would be an effective measure. These scenarios can be categorized as: (a) when crack opening is between zero to 0.03 inch, there is no need for the use of geosynthetics as a preventive method for reflection cracking, (b) when crack opening is between 0.03 to 0.07 inch, it is effective to use geosynthetics as a preventive measure for reflection cracking, and (c) when crack opening is larger than 0.07 inch, significant movement of cracked pavements makes geosynthetics unable to withstand the forces generated.

2.4 Methods to Evaluate Overlays

2.4.1 Introduction

The problem of reflection cracking in HMA overlays has been studied using different approaches including formulation of mechanistic models, numerical methods, and field and

laboratory experimentation. Several attempts have been made to address crack width and propagation since crack initiation and propagation are significant in understanding the process and mitigation of reflection cracking. The following sections summarize laboratory studies, field studies, and theoretical approaches to investigate reflection cracking, crack initiation and propagation.

2.4.2   Laboratory Methods for Testing HMA Mixes
2.4.2.1   Laboratory Devices to Study Reflection Cracking

Several laboratory devices have been developed to simulate field conditions for reflection cracking. One of the most cited tests in the reflection cracking research was developed in the Autun Laboratory in France (Vanelstraete and Francken 1997). The Texas overlay tester developed by Texas DOT in 2005 is another commonly used device in evaluating reflection cracking life of HMA overlays. Test results from the Texas overlay tester have been verified through more than five case studies in Texas and correlated well with the field performance. Lee et al. (2007) developed two set-ups in the laboratory to simulate reflection crack mechanisms as shown in Figure 2.3.
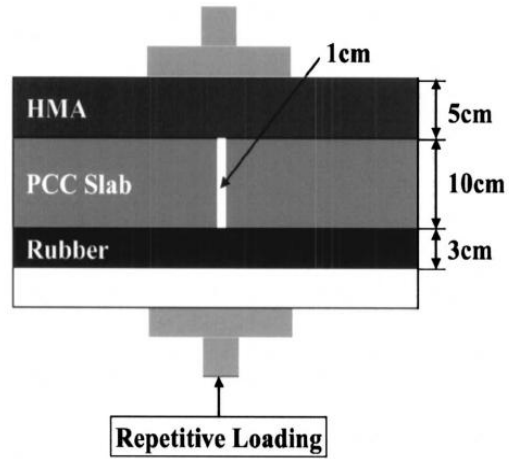
(a) Simulation of tensile strain
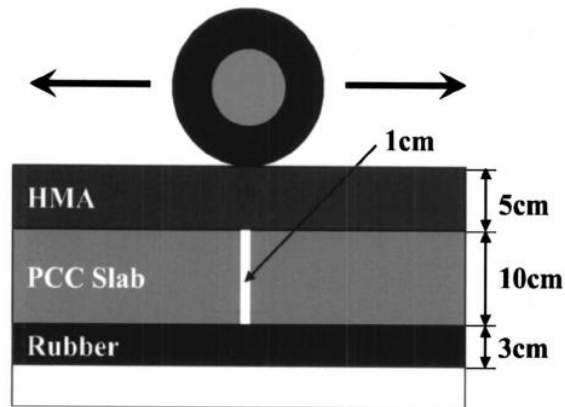
(b) Simulation of shear strain

(Lee et al. 2007)

FIGURE 2.3
Experimental Simulation of Tensile and
Shear Strains in HMA Overlays

The above-mentioned laboratory devices or set-ups are intended to simulate field conditions by creating simultaneous horizontal and vertical movements of jointed or cracked pavements thus creating tensile and shear strains at the bottom of HMA overlays.

2.4.2.2 Methods to Characterize Tensile Strength of HMA Mixture

Research has been conducted to characterize tensile strength of HMA mixtures and relate it to performance of asphalt pavements. Good understanding of fracture properties of HMA is essential to limit low-temperature cracking. Low temperature cracking is one of the factors responsible for reflection cracking. A high tensile strain at failure indicates a particular HMA can tolerate a higher strain before cracking, which means it is more likely to resist cracking than an HMA with a low tensile strain at failure. Tensile strengths of HMA before and after water conditioning can give some indication of moisture susceptibility. If a water-conditioned HMA sample retains most of its tensile strength as compared to a dry HMA sample, this HMA can be assumed reasonably moisture resistant. The simplest and most common test method to determine fracture resistance or tensile strength of a HMA mixture is the Marshall stability test. Although the Marshall stability test is simple, it cannot properly simulate field conditions; therefore, it has been abandoned in many countries. Currently, two test methods are commonly used to measure HMA tensile strength: (a) indirect tension test and (b) thermal cracking test. Researchers have used Indirect Tensile Tests (IDT) to characterize tensile properties of HMA mixtures (for example, Huang et al. 2003).

The IDT strength test was originally developed to measure the tensile strength of Portland concrete mixtures, and was later adopted to measure the tensile strength and modulus of asphalt concrete mixtures. Christensen (2003) showed a good relationship between laboratory IDT testing and field data. In the same research, the evaluation of IDT for measuring performance of HMA at low temperature was explored. Overall tensile stress for a ruggedness study was 415 psi with a standard deviation of 50.1 psi. These two results show that temperature plays a significant role in determining the tensile strength of HMA mixes. The procedure of the indirect tension test can be found in the AASHTO TP 9 standard "Determining the Creep Compliance and Strength of Hot Mix Asphalt (HMA) Using the Indirect Tensile Test Device".

The thermal cracking test determines the tensile strength and the temperature at fracture of an HMA specimen by measuring the tensile load in a specimen which is cooled at a constant rate while being restrained from contraction. This test is terminated when the specimen fails by

cracking. The procedure of the thermal cracking test can be found in the AASHTO TP 10 standard "Method for Thermal Stress Restrained Specimen Tensile Strength".

Measurement of tensile strain is important for evaluating the tolerable strain the HMA can endure before initiation and propagation of cracks at the bottom of HMA overlays and hence developing the reflection cracking. The most common method to measure the strain in an HMA specimen is attaching an extensometer at a specified location on the specimen. Recently, a more sophisticated method to measure strains in HMA specimens in the laboratory has been developed which uses image analysis (Masad et al. 2001). This method basically involves taking images of the HMA mix at various stages of a Georgia loaded wheel tester (GLWT) test by a charged couple device (CCD) camera and analyzing them with computer resources like the software MATCH. This software is used to calculate the translation and rotation of larger particles (smaller particles are considered part of the binder and eliminated manually at the image taking level) which have complex geometry. Analysis of images before and after the GLWT test gives the strain in the HMA.

In recent years, the semi-circular bend (SCB) test has been used in pavement engineering to characterize the tensile behavior of HMA mixtures. The SCB test is a fast and accurate three-point bending test to characterize the tensile strength of HMA specimens. Arabani and Ferdowsi (2007) pointed out that "the SCB test is going to be an accepted method for testing asphalt concrete pavements". The SCB test was adopted in this study of HMA overlays to characterize their tensile strengths.

2.4.2.3   Methods to Characterize Shear Strength of HMA Mixtures

As reflection cracking is a result of intolerable tensile strain and shear stress in HMA overlays, measurement of shear strength of HMA mixtures is equally important as measurement of the tensile strain. Researchers have used various laboratory methods and devices to study shear strength of HMA. Probably the most common device is Superpave Shear Tester (SST). The SST is a closed-loop system that can apply axial loads, shear loads, and confining pressures to asphalt concrete specimens at controlled temperatures. The response of asphalt concrete can be

used as input data for performance models. The SST is carried out in two ways, known as the repeated shear at a constant height (RSCH) test and the fixed shear at a constant height (FSCH) test. Abd El-Naby et al. (2002) introduced a test facility, which was used to assess the shear performance of HMA mixtures. They conducted a study on four different HMA mixtures and suggested correlation between shear strength and tensile strength. Wang et al. (2005) used a triaxial device to measure shear properties of HMA mixtures subjected to multi-stage loading. Chen et al. (2006) developed a uniaxial penetrating test to characterize the shear resistance of HMA mixtures and this test provided consistent data for selected HMA mixtures. However, these described techniques are sophisticated and unavailable to most researchers and engineers, thereby limiting their use of determining shear resistance characteristic of HMA mixtures.

In an attempt to develop a simple testing device for characterizing shear resistance of HMA mixtures, Wang et al. (2008) modified an MTS machine, the device consisting of two hollow cylinders of the same dimensions. HMA specimens with different diameters can be fitted between two cylinders. The two cylinders can move along a uniform plane under applied loading. Since the cylinders can move along the uniform plane, thereby inducing uniformly distributed shear stress at the middle part of the HMA specimen.

Since the SST is quite expensive and requires highly trained operators to run, a simplified version of the SST was developed through the National Cooperative Highway Research Program NCHRP project 9-7, known as the Field Shear Tester (FST). Sensitivity analysis of the FST showed that the values of complex modulus obtained from IDT and FST were quite similar (Christensen 2003).

2.4.2.4 Methods to Characterize Fatigue Behavior of HMA Mixtures

Fatigue behavior of HMA mixtures is one of the most significant factors for reflection cracking. Fatigue cracking is one of three main modes (fatigue cracking, rutting, and low temperature cracking) of early failure of HMA overlays and mainly caused by repetitive traffic loading on the pavements. The cracking resistance of HMA under repetitive loading is directly related to the behavior of HMA overlays under traffic loading. Therefore, characterizing the fatigue behavior of HMA mixtures in the laboratory has been a focus of research for many years.

Laboratory test methods are available to characterize the fatigue behavior of HMA mixtures. One of the most common laboratory test methods to characterize fatigue behavior of HMA mixtures is the beam fatigue test (Roberts et al. 1996). This test method is believed to possess most similar stress conditions to field HMA mixtures under repetitive traffic loading. This test is a three point loading method developed under SHRP-A-003A to evaluate the fatigue behavior of HMA mixtures. The beam fatigue test was modified in the SHRP-A-04 project to improve its simplicity and reliability. This fatigue test uses the pneumatic beam fatigue equipment, which has a beam specimen subjected to a repeated stress or strain-controlled loading. The load is applied at the center of the beam until the occurrence of failure. The test is digitally controlled and data is acquired through software. The failure is defined as a 50 percent reduction in initial stiffness, which is measured from the center point of the beam after the 50th load cycle (Roberts et al. 1996).

Recently, a new way to determine the failure of a flexural fatigue test was suggested by Carpenter et al. (2003) based on the dissipated energy concept (Ghuzlen and Carpenter 2000; Carpenter et al. 2003, and Shen and Carpenter 2005). In this method, the ratio of dissipated energy change is defined as a ratio of the change in the dissipated energy between two neighboring cycles divided by the dissipated energy of the first cycle.

2.4.3 Field Studies to Evaluate Crack Width

As the phenomenon of reflection cracking is complex and it involves several factors acting simultaneously, including traffic load, it is difficult to simulate the exact stress condition in the laboratory or using finite element models. Therefore, field studies have been carried out to closely examine the behavior of HMA overlays. The major drawbacks in full-scale field tests are that they are costly, time-consuming, and it is hard to control test conditions over a period of time.

In the field, the histogram-based machine vision was used to detect cracks ranging from 1/8 to 1 inch (3 to 25 mm) in width in both asphalt concrete (AC) and Portland cement concrete (PCC) pavements (Kirschke and Velinsky 1992).

Continuously reinforced concrete pavement (CRCP) is a concrete pavement constructed with continuous longitudinal steel reinforcement and no intermediate transverse contraction joints. Kohler and Roesler (2005) found that for a continuous reinforced concrete pavement (CRCP), the average measured crack width ranged from 0.0012 to 0.00457 inches (0.031 to 0.116 mm) at the steel depth at standard temperature. Kohler and Roesler (2006) measured the crack width near the surface varying between 0.001 and 0.0031 inches (0.0255 to 0.0777 mm) (at average pavement temperatures less than 10°C). During a 2-year period after construction, CRCP developed a transverse cracking pattern, with cracks typically spaced 2 to 6 ft (0.6 to 1.8 m) apart (Selezneva et al., 2003). Due to small crack width, it is generally not an issue for reflection cracks developed through HMA overlays on CRCP.

2.4.4 Theoretical Approaches to Study Reflection Cracking

Most of the methods to mitigate reflection cracking have been developed based on laboratory results and empirical formula, which produced results from very successful to disastrous. Since the 1970s, fracture mechanics theory has been used to analyze the fatigue behavior of HMA mixtures (Majidzadeh et al., 1971). Recent research has employed more favorable mechanistic approaches to determine fracture properties of HMA overlays using fracture mechanics theories. A fracture mechanics theory is used to understand the fundamental physical process taking place in the system. Complex geometry and complicated stress transfer often necessitate the use of finite element methods (FEM) and computer resources to solve a large system of equations. Molenaar (1993) evaluated the reflection cracking using FEM and fracture mechanics. De Bondt (1999) gave an extensive review of the phenomena of reflection cracking using FEM methods, fracture mechanics theories, as well as design procedures and the effectiveness of overlay alternatives. A new method called the Calibrated Mechanistic Approach with Surface Energy (CMSE) was developed by Walubita (2006) at the Texas A&M University for characterizing asphalt mixtures.

2.4.5 Theoretical Concepts to Address Crack Width

Normally crack analysis is done either by a smeared crack approach or a fracture mechanics approach. The basic principle of the fracture mechanics approach assumes the crack as a series of inter-connected single-line segments. Propagation of cracks from pre-existing defects through a material takes place according to certain crack growth criteria, such as the maximum energy release rate. On the other hand, the smeared crack approach assumes that cracks are spread over a finite region. An average tensile strain is the representation of crack presence over the concerned region. Using material models simulating proper compression and tension, cracking behavior of materials can be reasonably predicted by the smeared crack approach (Birgisson et al. 2003). However, no approach can fully capture the cracks propagating randomly through weak planes. "The explicit fracture model with the displacement discontinuity boundary element method has the potential to evaluate the mechanics of fracture in asphalt mixtures (Birgisson et al. 2003)". Figure 2.4 shows the general trend of crack propagation in HMA mixes based on the explicit fracture modeling.

Asphalt pavement fatigue cracking is an irreversible fracturing process caused by cyclic loading from traffic. Kumara et al. (2004) proposed a model to predict the distribution of longitudinal surface-initiated wheel path crack depths based on the cumulative equal single axle load (ESAL). In-service pavements selected for the study had large sample space. A stochastic relationship was also developed between the crack width/depth ratio and the cumulative ESALs based on the measurements obtained from a large number of core samples.
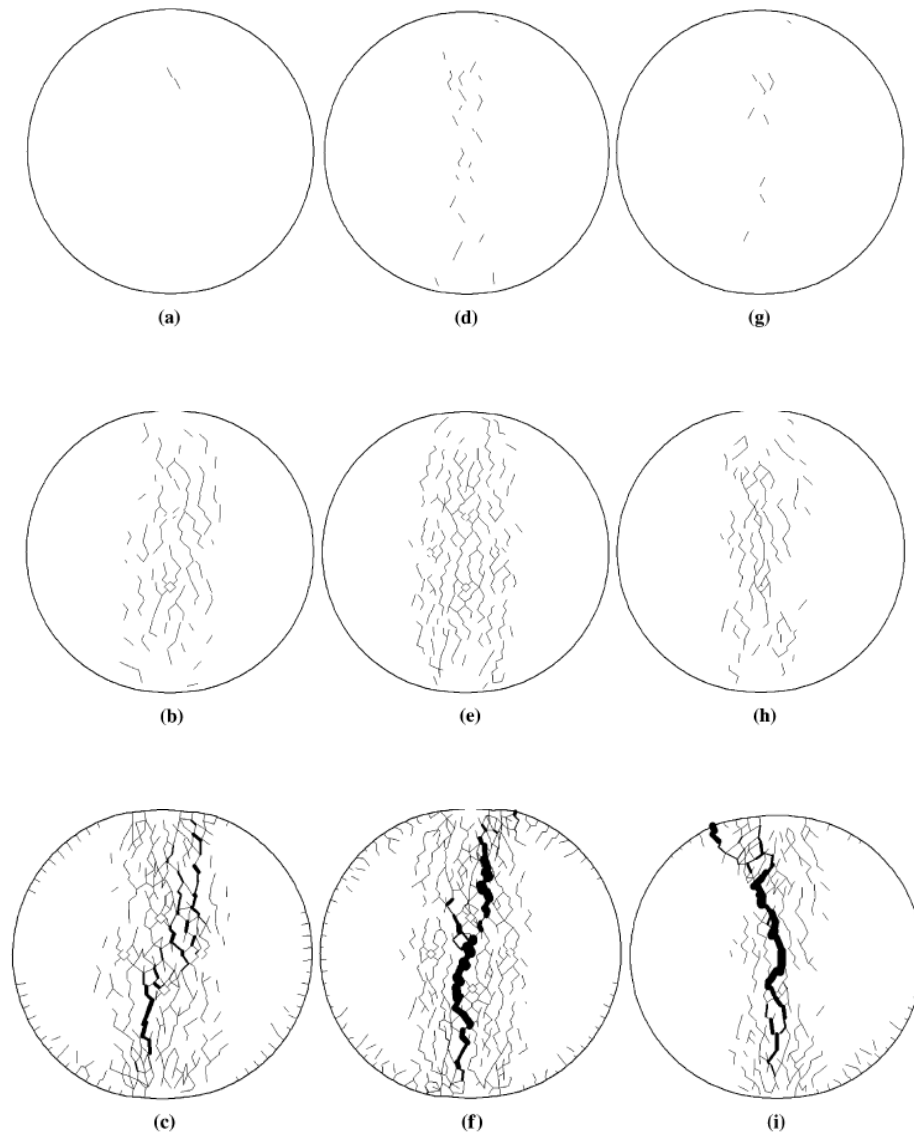
(Birginson et al. 2003)

FIGURE 2.4
Crack Propagation in Three Different Mixes: (a, d, g) First Crack
Appear, (b, e, h) Crack Pattern at Fracture Point, and (c, f, i)
Cracks at Final Load

In the earlier attempts to address the propagation of cracks through asphalt pavements, the concepts of fracture mechanics, Paris law, and J-integral have been used (Song et al., 2006). Castell et al. (2000) attempted to measure the crack growth experimentally. Recently, a cohesive zone model has been applied to address the fracture behavior of asphalt mixes and stimulate the propagation of cracks. With the help of the cohesive concept, a model was developed and

implemented with the help of the user-specified element in the ABAQUS software. A slender double cantilever beam was chosen and analyzed. The results from this cohesive zone model matched with the analytical solution even for small cracks (Song et al. 2006).

Chapter 3: Experimental Study

This chapter is comprised of four sections: (1) test equipment used in the study, (2) material characterization, (3) sample preparation, and (4) test procedure.

3.1 Test Equipment

This section describes different test apparatus that were used in this study.

3.1.1 Superpave Gyratory Compactor

The Superpave gyratory compactor is a transportable device. It is used to fabricate HMA specimens by simulating construction and traffic on an asphalt pavement. The level or amount of compaction is dependent on environmental conditions and traffic levels expected at a job site. The specimens fabricated with the gyratory compactor can be used to determine the volumetric properties (air voids, voids in the mineral aggregate, and voids filled with asphalt) of Superpave mixes. These properties, measured in the laboratory, indicate how well the mix meets design criteria. Thus a gyratory compactor can be used for quality control/quality assurance. This equipment can also be set up at a job site to verify that the delivered asphalt mix meets the job mix volumetric specifications.

To create a mix with a high degree of internal friction and high shear strength, the Superpave mix design procedures include requirements for aggregate angularity and gradation. The design goal is to produce a strong stone skeleton which resists rutting and to include enough asphalt and voids to improve the durability of the mix. Sample height, number of gyrations as well as pressure to be applied can be set in the Superpave gyratory compactor.

3.1.2 Direct Shear Box

A direct shear box is generally used to determine shear resistance of soil. The box is comprised of two rectangular sections placed on each other. A screw system can be used to adjust the spacing between two sections. When the top section is fixed with help of clamps, the lower section moves at a specified speed causing the shearing of the specimen prepared. Once the horizontal displacement of the lower moving box reaches a specified value, the test stops

automatically. The common issue in using a direct shear box to characterize shear resistance of soil is non-uniform distribution of shear stresses along the shearing surface (Brown et al. 2000). It is known that stresses at the corner are much more than those at the central part (DeBondt 1999). Since the HMA specimens used in this study were 1.5 and 2.0 inches thick, the non-uniformity of shear stresses across the samples should not be an important issue. Figure 3.1 shows the cross-sectional view of the direct shear box test with a vertically oriented HMA specimen supported by concrete blocks on both sides. A photo of the direct shear box is shown in Figure 3.2.
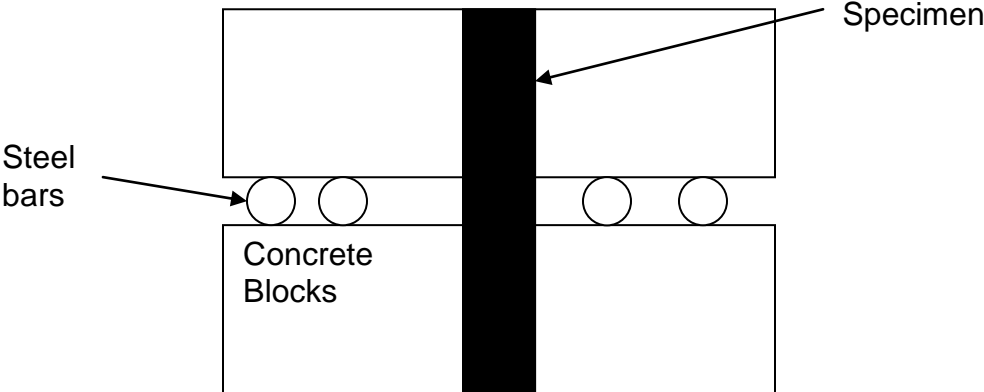
FIGURE 3.1
Cross-Sectional View of the Direct Shear Box with the HMA Specimen
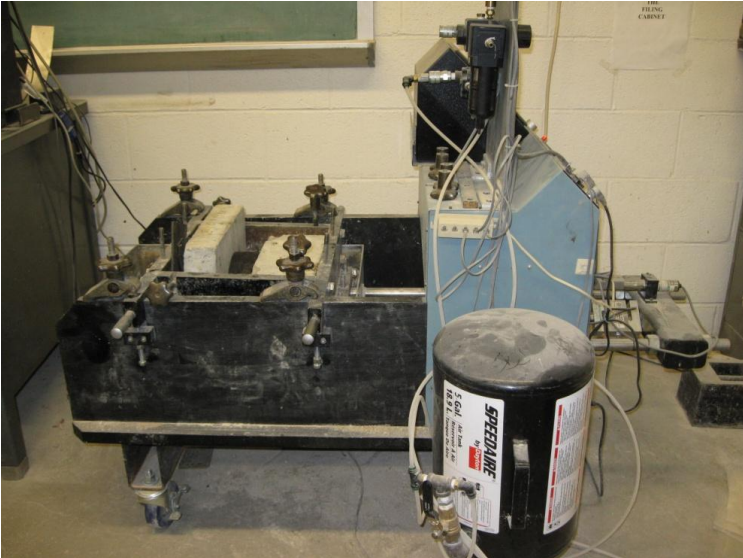
FIGURE 3.2
Direct Shear Box Test Used in the Study

3.1.3 Semi-Circular Bend Test Setup

The principle and basic setup of a semi-circular bend test to determine the tensile strength of an HMA sample is shown in Figure 3.3. The actual equipment used in this study is shown in Figure 3.4. Monotonic and cyclic loading can be applied to the semi-circular HMA specimen until failure. The loading rate for the monotonic loading on HMA samples is generally 2 in/min. The center to center distance between the two rollers is 80% of the sample diameter. The semi-circular bend test was previously used in rock mechanics to study the crack propagation and to determine tensile strength of rock. In recent years, several studies have been conducted to evaluate the tensile behavior of HMA mixes, for example, Krans et al. (1996), Molenaar et al. (2002), and Huang et al. (2005).
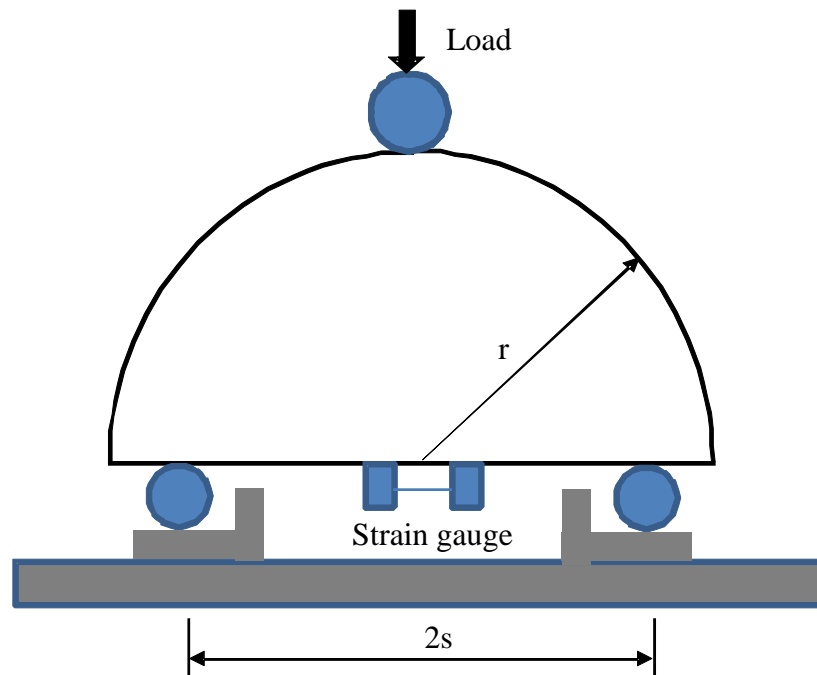
FIGURE 3.3
Systematic Diagram for Semi-Circular Bend Test
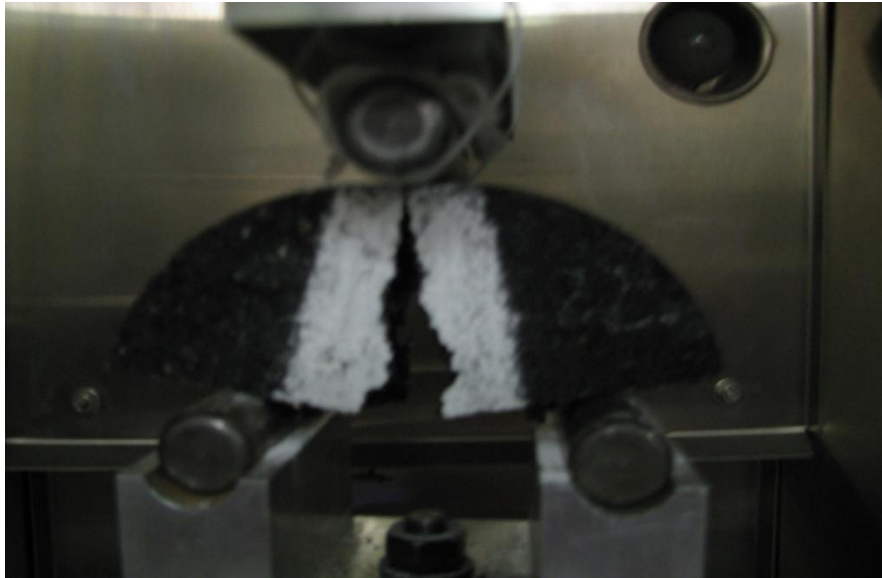
FIGURE 3.4
Semi-Circular Bend Test Setup

In Figure 3.3, r is the radius of the semi circular specimen, 2s is the center to center distance between support rollers. The diameter of the horizontal loading strip is 0.37 inch (9.4 mm) while the diameter of the two supporting strips is 0.25 inch (6.25 mm).

The maximum tensile stress at the bottom of the specimen can be calculated from the following equation, which was obtained from a finite element analysis (Molenaar et al. 2002 and Huang et al. 2005):

$$\sigma_x = 3.564 \frac{P_{ult}}{Dt}$$ **Equation 3.1**

where

σ_x = maximum tensile stress (MPa)

P_{ult} = peak load (N)

t   = thickness of the specimen (mm)

D   = diameter of the specimen (mm)

21

3.1.4 Overlay Loading Test Setup

A loading apparatus designed and fabricated at the geotechnical laboratory at the University of Kansas was used for the overlay loading test. The loading system had a reaction frame and a base plate made of steel sections and a 6 inch diameter air cylinder with a maximum air pressure of 130 psi. However, the available air pressure supply of 100 psi at the lab was used during the test. An arbitrary waveform generator Model 75 was used to control the loading system and apply the cyclic loading. The waveform generator was used to control the frequency of loading cycles, the maximum and minimum loads, and the number of loading cycles. A smart dynamic strain recorder DC-204R was used to record the data from all the strain gage type sensors.

The details of the test setup are shown in Figure 3.5. A 2 inch thick rubber pad was placed on the loading platform to simulate a subgrade. Two 4 inch thick concrete blocks with a plan dimension of 13 x 10.6 inches were placed on the rubber pad. These concrete blocks were cast and cured for 28 days before the test and they are movable and were set to create a gap between concrete blocks at 0.2, 0.4, or 0.6 inches. A 1.5 or 2 inch thick HMA slab with a plan dimension of 21 x 12 inches was fixed on top of the concrete blocks by Emulsion Bonding Liquid (EBL) asphalt emulsion as a tack coat material to simulate an overlay as shown in Figure 3.6. The application rate of the EBL was approximately 0.15 gal/yd^2. After the test specimen was set up, a displacement transducer was installed horizontally at the bottom of the HMA overlay to measure strains during each cyclic test as shown in Figure 3.7. A steel cylindrical tube filled with concrete as shown in Figure 3.8 was 4 inches in diameter and 12 inches in length and used to apply a load on the test specimen. The length of the tube was identical to the width of the HMA slab. Figures 3.9 and 3.10 show the loading frame, cylinder, displacement transducers, controller, and data recording system.
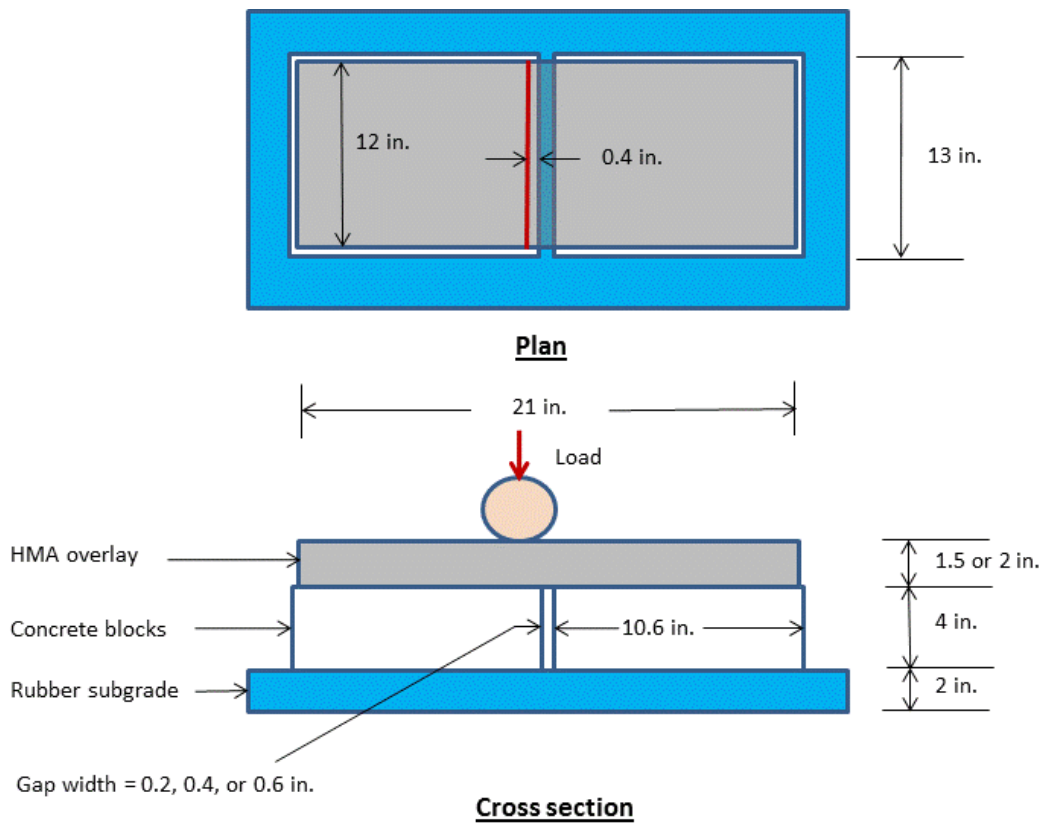
FIGURE 3.5
Plan and Elevation Views of the Overlay Loading Test Setup

FIGURE 3.6
Application of EBL Tack Coat before Placing an HMA Overlay

FIGURE 3.7
A Displacement Transducer Affixed on the HMA Overlay

FIGURE 3.8
Picture of the Cylinder Used for Loading with the Displacement Transducer to Measure the Vertical Displacement
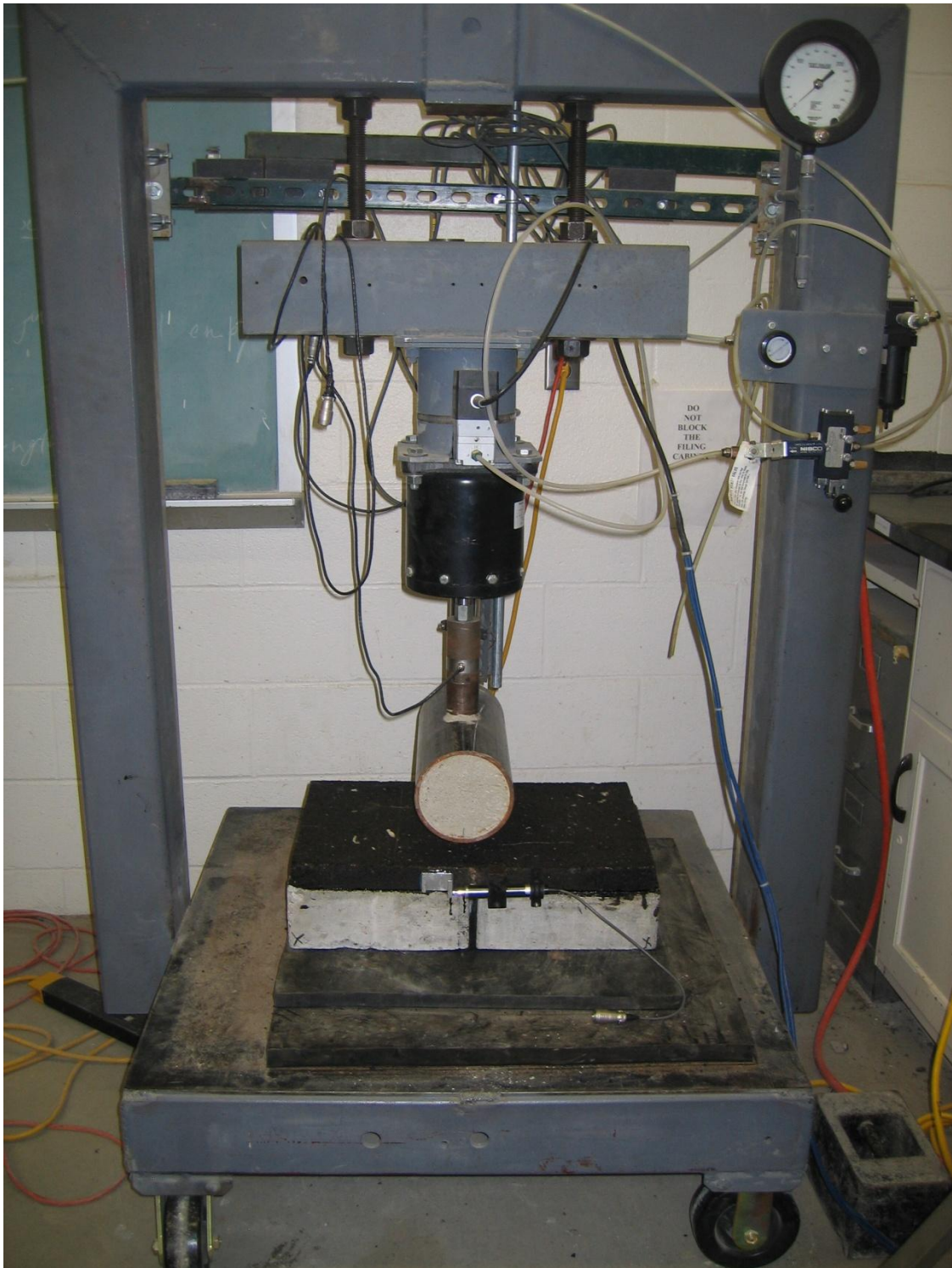
FIGURE 3.9
Picture of the Test Specimen and Loading System

FIGURE 3.10
Picture of the Test Setup Including the Loading
System, Controller, and Data Recording System

3.2 Material Characterization

Materials from two of KDOT's projects, namely 089 C-4318-01 (Mix 1) and 56-29 KA-1087-01 (Mix 2), were selected for this study. Mix design SM 12.5 A was used for both mixes. Direct shear box and semi-circular bend tests were conducted on both mixes while overlay loading tests were conducted on Mix 1 only.

3.2.1 Asphalt Binder

Bitumen used for the HMA specimens was from Hamm, Inc. (HMA Contractor). Two types of binder, PG 64-22 and PG 76-22, were chosen for this study, in which PG 64-22 binder was used for Mix 1 while PG 76-22 was used for Mix 2. The specific gravity values of these two asphalt binders were 1.041 and 1.040, respectively. The recommended asphalt content for Mix 1 was 6.25% and that for Mix 2 was 5.6%.

3.2.2 Aggregate and Mix Design Specification
3.2.2.1 HMA Mix 1

The percent of aggregates used in HMA Mix 1 and their specific gravity values are provided in Table 3.1. The sieve analysis of the aggregates used in HMA Mix 1 is provided in Table 3.2. Figure 3.11 shows the gradation of aggregates used to make the test specimens for Mix 1. The mix design specification for Mix 1 is presented in Table 3.3. Parameters for the preparation of specimens for HMA Mix 1 are provided in Table 3.4.

TABLE 3.1
Percent of the Aggregates Used in HMA Mix 1 and Their Specific Gravity Values

Aggregate designation	Percent in Mix	Specific Gravity
CS-1	12	2.518
CS-1A	34	2.521
MSD	43	2.538
SSG	11	2.599
Binder PG 64-22	Total= 100	Combined aggregate specific gravity = 2.536

TABLE 3.2
Sieve Analysis of the Aggregates Used in HMA Mix 1

Sieve size	CS-1 (% retained)	CS-1A (% retained)	MSD (% retained)	SSG (% retained)
¾"	0	0	0	0
½"	64	0	0	0
3/8"	95	13	0	0
No. 4	97	81	0	0
No. 8	98	97	30	11
No. 16	98	97	60	32
No. 30	98	97	81	62
No. 50	98	97	91	90
No. 100	98	97	94	98
No. 200	98	97	95	99.5
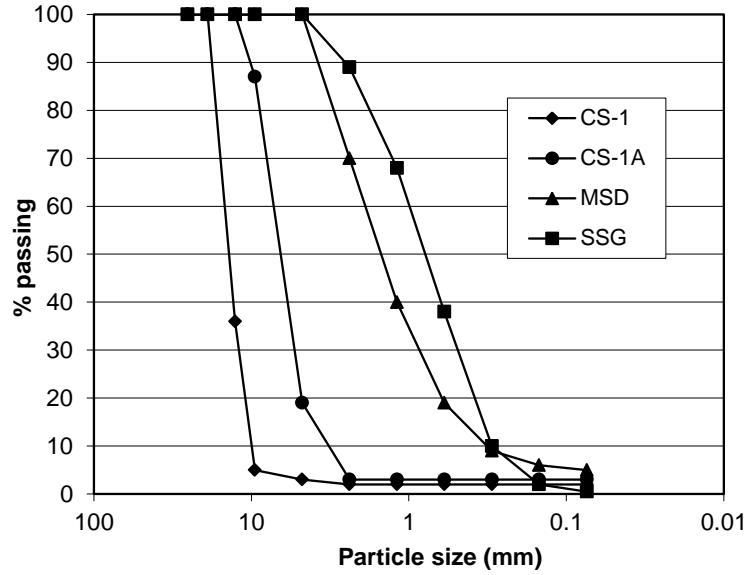
FIGURE 3.11
Aggregate Gradations Used for Test Specimens (Mix 1)

TABLE 3.3
Mix Design Specification for Mix 1

Asphalt content (%)	6.250
% Aggregate by mass of mix	93.75
Specific gravity of asphalt	1.041
Bulk specific gravity of aggregate	2.536
Max specific gravity	2.410
Bulk specific gravity of mix	2.310
Effective specific gravity of aggregate	2.641
Absorbed AC (%)	1.632
Effective AC (%)	4.720
% VMA	14.6
% Air voids	4.15
% VFA	72
Effective film thickness	10.73
Dust/binder ratio	1.1

TABLE 3.4
Parameters for the Preparation of HMA Mix 1 Specimens

Mix design	SM 12.5A
Mixing temperature range (^{o}F)	302-313
Molding temperature range (^{o}F)	282-291
N_{ini} gyrations	7
N_{design} gyrations	75
N_{max} gyrations	115
Asphalt content (%)	6.25

3.2.2.2 HMA Mix 2

The percentage of aggregates used in HMA Mix 2 and their specific gravity values are presented in Table 3.5. The sieve analysis of aggregates used in HMA Mix 2 is presented in Table 3.6 and Figure 3.12. The mix design specification for Mix 2 is presented in Table 3.7. Parameters for the preparation of specimens for HMA Mix 1 are provided in Table 3.8.

TABLE 3.5
Percent of the Aggregates Used in HMA Mix 2 and their Specific Gravity Values

Aggregate designation	Percentage in Mix	Specific Gravity
CG-1	20	2.578
CG-2	25	2.581
CG-3	25	2.581
SSG-2	30	2.594
Binder PG 76-22	Total= 100	Combined Aggregate Specific Gravity = 2.584

TABLE 3.6
Sieve Analysis for the Aggregate Used in HMA Mix 2

Sieve size	CG-1 (% retained)	CG-2 (% retained)	CG-3 (% retained)	SSG-2 (% retained)
3/4	0	-	-	0
1/2	36	0	0	2
3/8	70	0	0	4
4	96	10	11	13
8	97	40	43	41
16	98	57	62	70
30	98	67	74	85
50	98	76	83	95
100	98	84	91	99
200	98.2	91	95	99.2
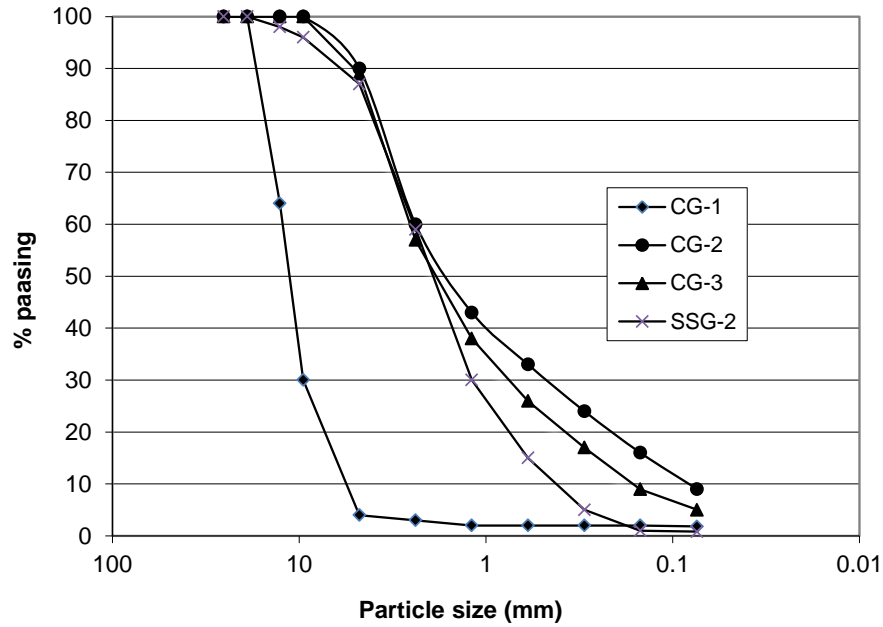
FIGURE 3.12
Aggregate Gradations Used for Test Specimens (Mix 2)

TABLE 3.7
Mix Design Specification for Mix 2

Asphalt content	5.50
% Aggregate by mass of mix	94.500
Specific gravity of asphalt	1.0400
Bulk specific gravity of aggregate	2.584
Maximum specific gravity	2.408
Bulk specific gravity of mix	2.292
Effective specific gravity of aggregate	2.613
Absorbed AC (%)	0.447
Effective AC (%)	5.078
%VMA	16.2
% Air voids	4.82
% VFA	69
Effective film thickness	10.32
Dust/binder ratio	0.7

TABLE 3.8
Parameters for the Preparation of HMA Mix 2 Specimens

Mix design	SM 12.5A
Mixing temperature range (F)	310-340
Molding temperature range	295-320
N_{ini} gyrations	8
N_{design} gyrations	100
N_{max} gyrations	160
Asphalt content (%)	5.6

3.2.3 Rubber Subgrade

A 2 inch thick rubber pad was used in the HMA overlay loading tests to simulate a subgrade. Two static loading tests were conducted on a 6 inch diameter steel plate on the rubber pad to evaluate the stress-strain response. Figure 3.13 shows the stress-strain curve of the rubber pad. The two tests yielded close results. Based on the linear portion during loading (from 20 to 100 psi) or the rebound curve during unloading (from 100 to 0 psi), the elastic modulus of the rubber subgrade was calculated to 3,330 psi.
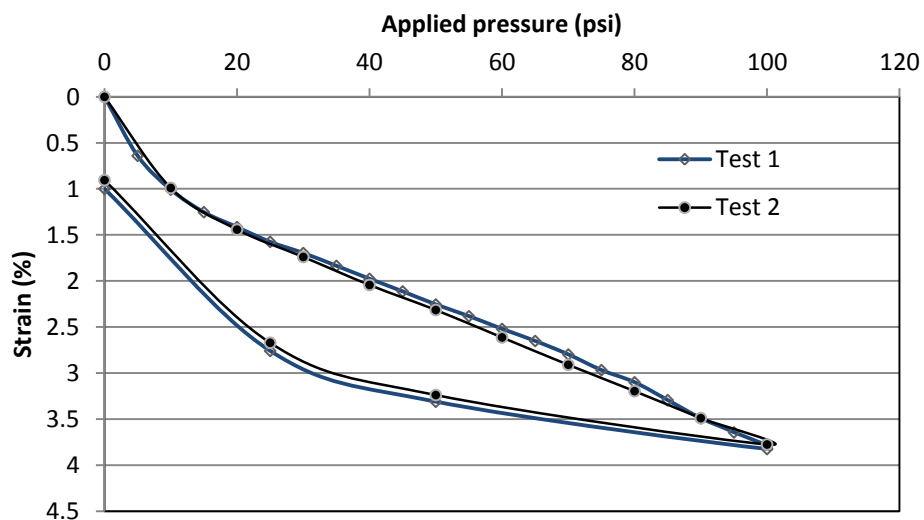
FIGURE 3.13
Stress-Strain Curve of the Rubber Subgrade

3.3 Sample Preparation

Cylindrical samples were prepared for direct shear and semi-circular bend (SCB) tests. Diameter of all the samples was 6 inches. Each set of samples had two thicknesses: 1.5 and 2.0 inches. All samples were prepared at KU using the Superpave gyratory compactor. Two types of mixes (Mix 1 and Mix 2) were used for this study. The asphalt binder contents used in this study were 6.25 % for Mix 1 and 5.6 % for Mix 2, respectively.

Mix and compaction temperatures were selected based on the requirements of the KDOT design as shown in Tables 3.4 and 3.8. Aggregates were weighed and heated in an oven to the desired mix temperature and then mixed with binder in a mechanical mixer. A hand scoop was

also used to mix and to make sure aggregates were mixed properly. The mix was then heated in an oven for two hours for short term aging.

The Pine Superpave gyratory compactor was used to compact the specimens. Gyratory molds, the mix pouring funnel and the scoop were all heated to the compaction temperature. After two hours of short-term aging, the required quantity of HMA mix for one specimen was poured in the gyratory mold using the pouring funnel. The mold was then placed inside the gyratory compactor chamber and the door was closed. The number of gyrations, the specimen height, and the required compaction pressure were set on the control panel. In this study, the compaction pressure was set at 87 psi and the number of gyrations was set at 75 and 100 for Mix 1 and Mix 2, respectively. The base of the compactor inclined to 1.25° and the load was applied from upper and lower plates. The compactor stopped itself when either the set height or the number of gyrations was reached. Once the machine self parked, the door was opened and the compacted specimen was removed from the chamber and extruded using the hydraulic jack on the side of the compactor. Some of the prepared specimens are shown in Figure 3.14.

The HMA overlay slabs were prepared by KDOT using Mix 1 and the Linear Kneading Compactor at the Material and Research Center's asphalt laboratory.

FIGURE 3.14
Prepared HMA Specimens

3.4 Test Procedure

This section describes the test procedures for the direct shear box test, the semi-circular bend test, and the overlay loading test.

3.4.1 Direct Shear Box Test

A circular specimen prepared by the Superpave gyratory compactor was placed into the direct shear box. With the help of concrete blocks, bending of the HMA specimen was restricted. Steel bars were placed between the upper and lower portions of concrete blocks as shown in Figure 3.15 to create spacing which simulates the gap width in underlying cracked concrete slabs. Figure 3.16 shows the complete setup of the specimen. Once the specimen was set up, a shearing speed was set at 0.1 in/min and a maximum horizontal displacement was set to be 1 inch as a safety measure for the machine, with the help of the control panel. Data acquisition was done by the WINSAX program. Once all the required parameters were set up, the WINSAX application was opened in the computer. This application required various parameters to be checked and details about the specimen to be added. Both the START button on the direct shear box and the RUN button in the consol were pressed at the same time. The test started and data was recorded after 10 sec. The test ran until the horizontal displacement of the lower section of the direct shear box reached 0.5 inch. After that, the test stopped and a file was saved in the folder on the computer. All the tests were conducted at room temperature, 25 ± 1°C. Figure 3.17 shows the appearance of the specimen after failure.

FIGURE 3.15
Concrete Blocks and Steel Bars with an HMA Specimen

FIGURE 3.16
The HMA Specimen between Lower and Upper Concrete Blocks

FIGURE 3.17
The Failed Specimen after the Direct Shear Box Test

3.4.2 Semi-Circular Bend Test

All the semi-circular bend (SCB) tests were conducted at the transportation material lab at the University of Tennessee. Both static and cyclic fatigue tests were conducted on HMA specimens. The test procedure is described below for both cases. All the tests were conducted at room temperature, 20±1°C. Figure 3.18 shows the setup for a semi-circular bend test. A white patch was made in the middle of the specimen surface with chalk to assist better visual aid in recognizing the first crack appearance during the cyclic test. An extensometer was attached at the bottom of the specimen to measure strains.

FIGURE 3.18
A Semi-Circular Bend Test with an Extensometer Attached
at the Bottom of the Specimen

3.4.2.1 Procedure for a Static SCB Test

Step 1: Set the loading rate in the MTS machine at 2 in/min.

Step 2: Attach the extensometer at the bottom of the specimen.

Step 3: Place the semi-circular HMA test specimen to the holding frame (specifically made for SCB tests) attached to the MTS machine.

Step 4: Check all the connections and launch the software to control the loading and record the test data.

Step 5: Start loading the specimen.

Step 6: When the specimen fails, stop the test.

3.4.2.2 Procedure for a Cyclic Fatigue SCB Test

Step 1: Set the loading pattern in the MTS machine having a frequency of 1.0 Hz. The loading pattern follows 0.05 sec loading, 0.05 sec unloading, and rest for 0.9 sec.

Step 2: Set the load at a fraction (80%, 70%, 60%, 50%, 40%, and 30%) of the maximum compressive load from the static load tests.

Step 3: Attach the extensometer at the bottom of specimen.

Step 4: Place the semi-circular HMA test specimen to the frame attached to MTS machine

Step 5: Check all the connections and launch the software to control the loading and record the test data.

Step 6: Start loading the specimen.

Step 7: Once the extensometer reaches the limit (from which it would not record any data) before the specimen fails (visual inspection), stop the MTS machine and adjust the extensometer so that more data could be recorded) and re-start the test.

Step 8: When the specimen failed, stop the test.

3.4.3 Overlay Loading Tests

A static loading test was first performed to determine the maximum load capacity of the HMA overlay. The load was applied in increments until the failure of the overlay. The vertical displacement of the loading cylinder and the horizontal deformation of the overlay were monitored during the test.

After the static loading test, a series of cyclic loading tests were conducted at a load in a percentage of the load corresponding to the initiation of the crack on the HMA overlay.

All the static and cyclic loading tests were conducted at room temperature, $20\pm1°C$. The bottom line of the loading cylinder was located close to the inner edge of one concrete block.

Chapter 4: Test Results and Discussion

This chapter is comprised of two sections dealing with (a) test results obtained from direct shear box tests, semi-circular bend tests, and overlay loading tests and (b) analysis and discussion of test results.

4.1 Test Results

Results from direct shear box tests, semi-circular bend tests, and overlay loading tests on gapped concrete blocks are presented in this section.

4.1.1 Direct Shear Tests

Direct shear tests were conducted on HMA Mix 1 and Mix 2 specimens with thicknesses of 1.5 and 2.0 inches. To simulate the crack width on existing concrete pavements in field, three different gaps (0.25, 0.375, and 0.5 inches) between concrete blocks were created by steel rods of different diameters. Totally, nine tests were conducted for each mix at one specimen thickness, in which three tests were done at each gap. Figures 4.1 and 4.2 show the typical load-displacement curves for Mix 1 and Mix 2 specimens. It is shown that the shear load increased with the horizontal displacement and reached the maximum load before decreasing. The measured maximum shear loads for Mix 1 and Mix 2 specimens with thicknesses of 1.5 and 2.0 inches are tabulated in Tables 4.1 to 4.4.
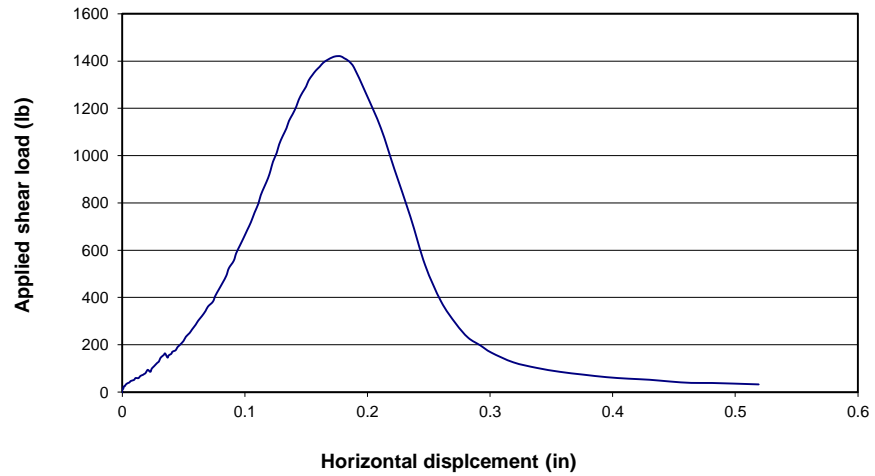
FIGURE 4.1
A Typical Load-Displacement Curve for the 2.0 Inch Thick Mix 1 Specimen (Gap Width = 0.25 Inch)
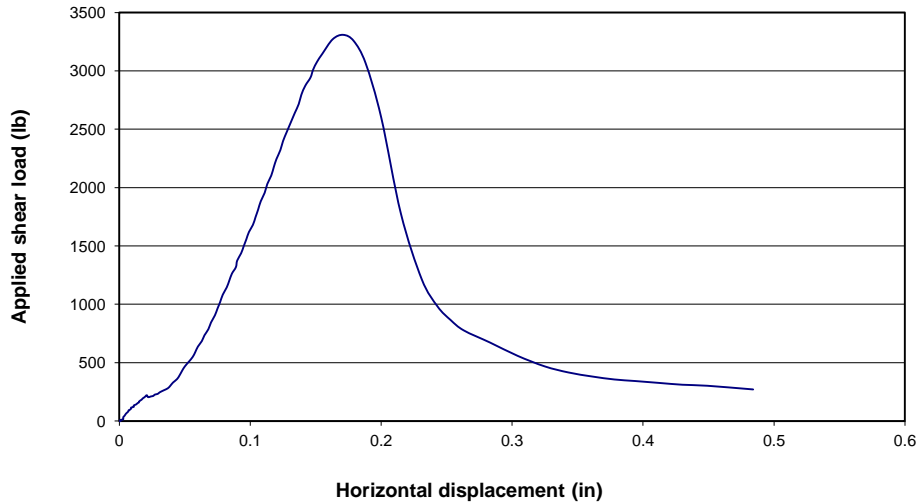
FIGURE 4.2
A Typical Load-Displacement Curve for the 2.0 Inch Thick Mix 2 Sample (Gap Width = 0.25 Inch)

TABLE 4.1
Maximum Shear Loads by Direct Shear Tests for 1.5 Inch Thick Mix 1 Specimens

Specimen #	Gap Width (inch)	Bulk Sp. Gr.	Maximum Load (lb)
1	0.5	2.214	1117
2	0.5	2.199	897
3	0.5	2.199	1092
4	0.375	2.221	1194
5	0.375	2.230	1161
6	0.375	2.251	1353
7	0.25	2.143	852
8	0.25	2.191	928
9	0.25	2.180	989

TABLE 4.2
Maximum Shear Loads by Direct Shear Tests for 2.0 Inch Thick Mix 1 Specimens

Specimen #	Gap Width (inch)	Bulk Sp. Gr.	Maximum Load (lb)
1	0.5	2.285	1829
2	0.5	2.265	1825
3	0.5	2.230	1385
4	0.375	2.245	1774
5	0.375	2.244	1366
6	0.375	2.257	1536
7	0.25	2.196	1100
8	0.25	2.191	1633
9	0.25	2.223	1421

TABLE 4.3
Maximum Shear Loads by Direct Shear Tests for 1.5 Inch Thick Mix 2 Specimens

Specimen #	Gap Width (inch)	Bulk Sp. Gr.	Maximum Load (lb)
1	0.5	2.263	2511
2	0.5	2.306	2333
3	0.5	2.294	2412
4	0.375	2.310	2305
5	0.375	2.303	2484
6	0.375	2.301	2368
7	0.25	2.291	2816
8	0.25	2.264	2131
9	0.25	2.278	2696

TABLE 4.4
Maximum Shear Loads by Direct Shear Tests for 2.0 Inch Thick Mix 2 Specimens

Specimen #	Gap Width (inch)	Bulk Sp. Gr.	Maximum Load (lb)
1	0.5	2.377	3073
2	0.5	2.365	3385
3	0.5	2.356	3347
4	0.375	2.370	3083
5	0.375	2.366	2968
6	0.375	2.316	2685
7	0.25	2.323	2801
8	0.25	2.340	3135
9	0.25	2.340	3307

4.1.2 Semi-Circular Bend Tests

Semi-circular bend tests were conducted on specimens of both mixes at thicknesses of 1.5 and 2.0 inches under static and cyclic loading. A constant displacement rate at 2 inches/min was applied for the static load tests. A sinusoidal loading (0.05 sec loading, 0.05 sec unloading, and 0.9 sec rest period) of frequency 1 Hz was applied for the cyclic tests. Amplitude of sinusoidal loading was a fraction of the maximum compressive load obtained from the static tests. Strains were measured at the bottom of the specimen with a help of an extensometer attached to each specimen. All the data acquisition was done with the help of MTS software. The wave pattern of cyclic loading is shown in Figure 4.3.
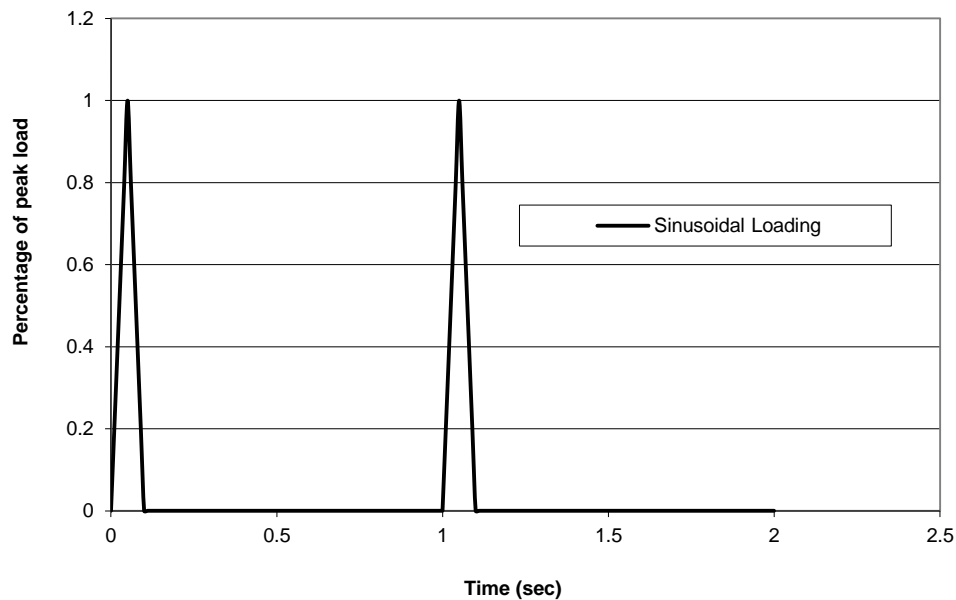
FIGURE 4.3
Loading Pattern Used for Cyclic Semi-Circular Bend Tests

For each static loading test, the maximum or peak compressive load a specimen could take and the strain induced at the bottom of the HMA semi-circular specimen were recorded. Figures 4.4 and 4.5 show the typical compressive load vs. strain curves from static loading tests on two specimens at thicknesses of 1.5 and 2.0 inches The static test results for Mix 1 and Mix 2 specimens are tabulated in Tables 4.5 and 4.6. It is shown that the Mix 2 specimens had higher maximum loads than the Mix 1 specimens.
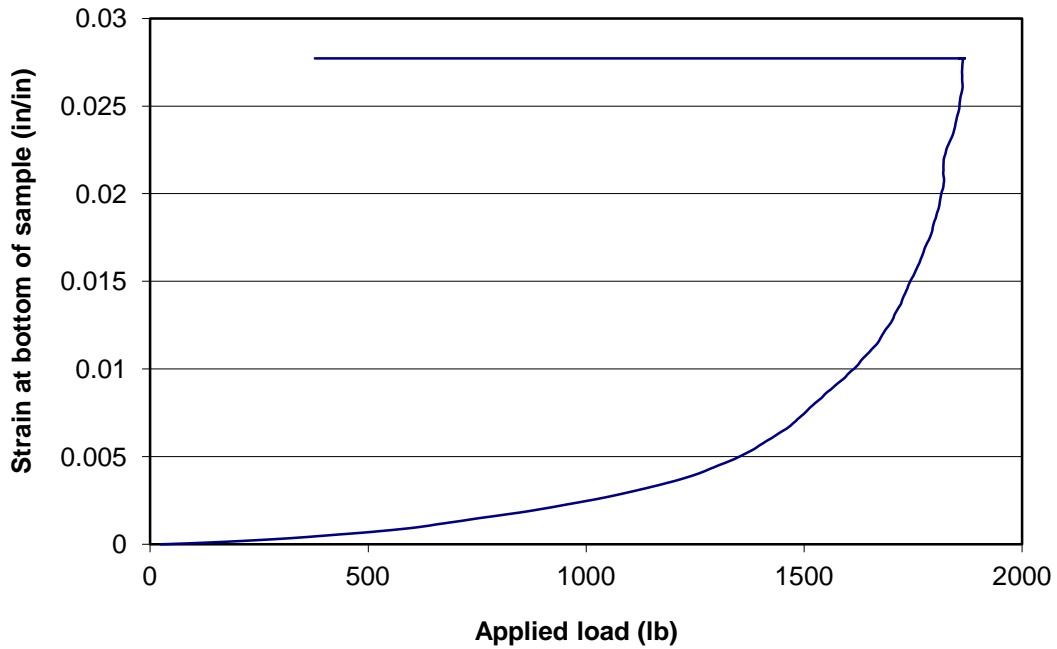
FIGURE 4.4
The Applied Compressive Load versus the Strain Developed at the Bottom of the 2.0 Inch Thick Mix 1 Specimen
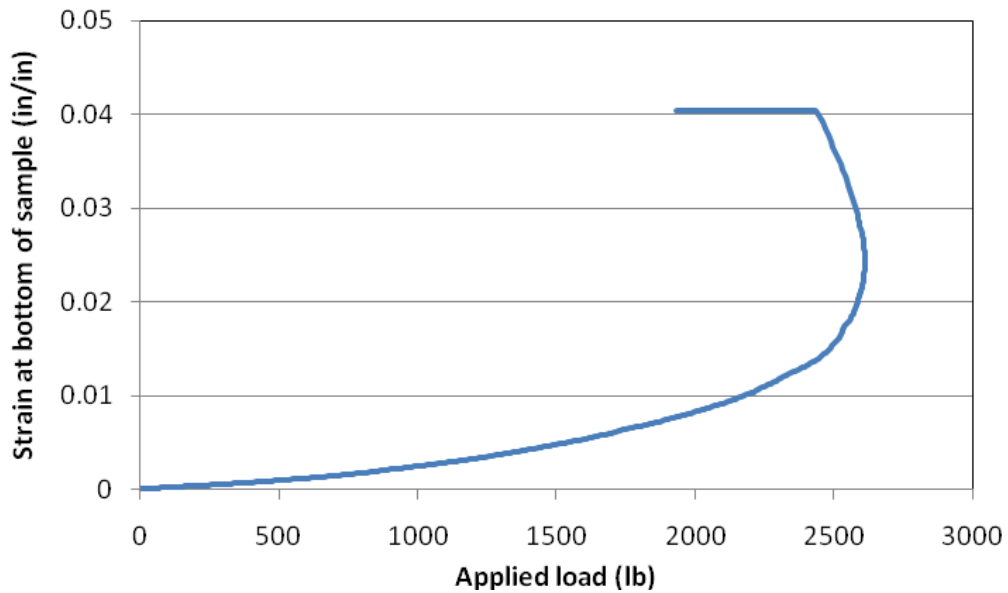
FIGURE 4.5
The Applied Compressive Load versus the Strain Developed at the Bottom of 1.5 Inch Thick Mix 2 Specimen

TABLE 4.5
Static Test Results for Mix 1

Specimen #	Thickness (inch)	Bulk Specific Gravity	Maximum Load (lb)	Average Maximum Load (lb)
1	1.5	2.214	1650	1547
2	1.5	2.220	1444	
3	2.0	2.197	1868	2072
4	2.0	2.218	2276	

TABLE 4.6
Static Test Results for Mix 2

Specimen #	Thickness (inch)	Bulk Specific Gravity	Maximum Load (lb)	Average Maximum Load (lb)
1	1.5	2.300	2244	2449
2	1.5	2.287	2494	
3	1.5	2.287	2610	
4	2.0	2.354	4174	4145
5	2.0	2.360	3932	
6	2.0	2.370	4328	

Cyclic semi-circular bend tests were conducted at a fraction of the average maximum

compressive load obtained from the static tests for Mix 1 and Mix 2. The pattern of one load

cycle is shown in Figure 4.3 while the typical pattern of load cycles for a complete test is shown

in Figure 4.6. The strains at the bottom of each specimen with time were measured continuously.

Figure 4.7 shows a typical example of the strain vs. test time curve.
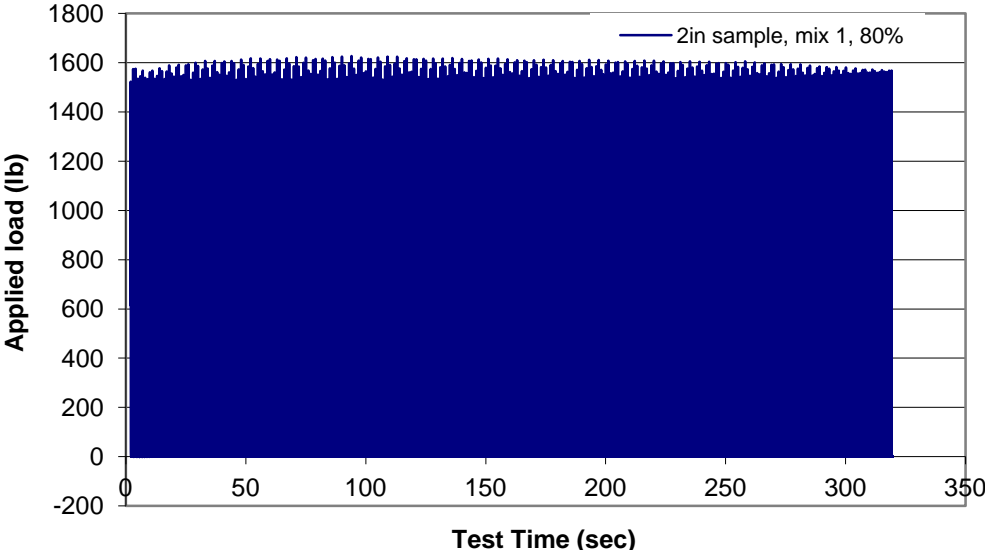
FIGURE 4.6
Cyclic Loading for a Semi-Circular Test of a 2.0 Inch Thick Mix 1
Sample at 80% Static Maximum Load
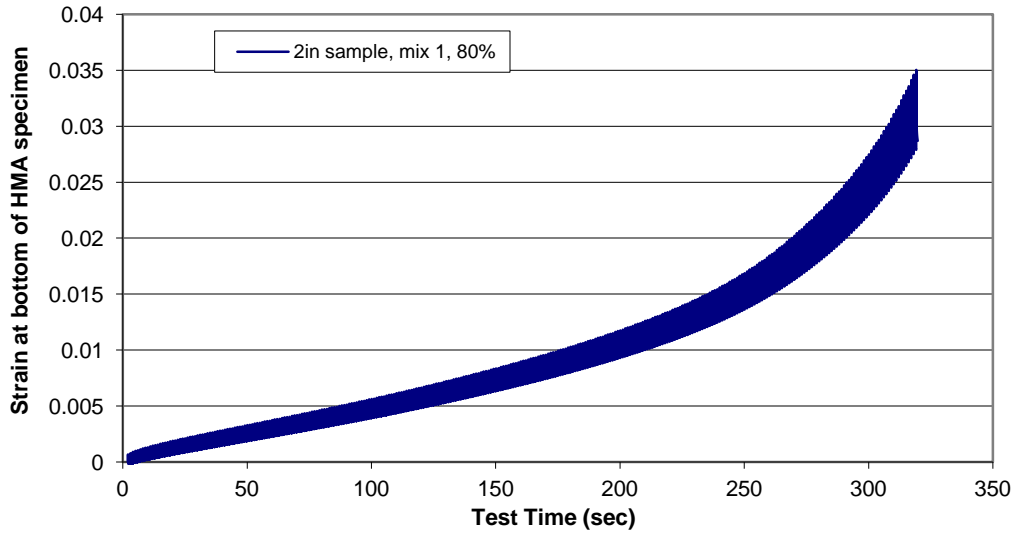
FIGURE 4.7
Strains Developed at the Bottom of the Specimen versus the Test
Time for a 2.0 Inch Mix 1 Specimen at 80% Static Maximum Load

Tables 4.7 and 4.8 summarize the test results of Mix 1 and Mix 2 specimens, respectively under cyclic semi-circular bend tests, including the thickness, specific gravity, % static maximum load, applied maximum load, time when the initial crack was observed, and total test time.

TABLE 4.7
Static Test Results of Semi-Circular Bend Tests for Mix 1 Specimens

Specimen #	Thickness (inch)	Specific gravity	% static max. load	Applied max. load (lb)	Initial crack (sec)	Test time (sec)
1	1.5	2.212	80	1200	34	74
2	1.5	2.241	70	1050	220	412
3	1.5	2.221	60	900	37	72
4	1.5	2.245	50	750	224	415
5	1.5	2.213	40	600	818	1298
6	1.5	2.232	30	450	820	1822
7	2.0	2.217	80	1600	296	341
8	2.0	2.229	70	1400	330	374
9	2.0	2.231	50	1000	1258	1637
10	2.0	2.246	50	1000	1133	1411
11	2.0	2.236	30	600	11170	13475

TABLE 4.8
Cyclic Test Results of Semi-Circular Bend Tests for Mix 2 Specimens

Specimen #	Thickness (inch)	Specific gravity	% static max. load	Applied max. load (lb)	Initial crack (sec)	Test time (sec)
1	1.5	2.304	80	1960	10	18
2	1.5	2.296	70	1715	175	173
3	1.5	2.277	60	1470	695	431
4	1.5	2.322	50	1225	355	369
5	1.5	2.289	50	1225	170	182
6	1.5	2.293	40	980	968	1216
7	1.5	2.274	30	735	3848	4951
8	2.0	2.392	80	3315	63	65
9	2.0	2.378	70	2901	140	169
10	2.0	2.377	60	2486	150	180
11	2.0	2.375	50	2072	645	691
12	2.0	2.333	40	1658	673	733
13	2.0	2.393	30	1243	6274	6827

4.1.3 Overlay Loading Tests

One static loading test was conducted before the cyclic loading tests to the maximum load capacity of the 2.0 inch thick HMA overlay on gapped concrete blocks. In this test, the gap between the two concrete blocks was 0.4 inch. The HMA overlay is considered failed after the vertical cracks on the sides of the HMA specimen propagated through the overlay thickness. The static loading test was run to a maximum load of 6,500 lb/ft; however, a load of 3,000 lb/ft caused the HMA overlay to fail. Figure 4.8 shows the vertical displacement of the HMA overlay on the gapped concrete blocks and the rubber subgrade while Figure 4.9 shows the horizontal deformation of the HMA overlay within a gauge length of 2 inches. The horizontal strain (also tensile strain) was calculated based on the measured horizontal deformation on the HMA overlay divided by the gauge length as shown in Figure 4.10. After the applied load reached 3,000 lb/ft, the overlay started to bend and crack lines were visible right on top of the gap between the two concrete blocks. From the static loading test, the failure load was found to be 3000 lb/ft when the main vertical crack line on the sides of the HMA overlay reached the top surface. The HMA overlay started to be lifted up at the edges after the applied load more than 4,000 lb/ft as shown in Figure 4.11. Figure 4.12 shows the crack lines on the HMA overlays after the static loading test.
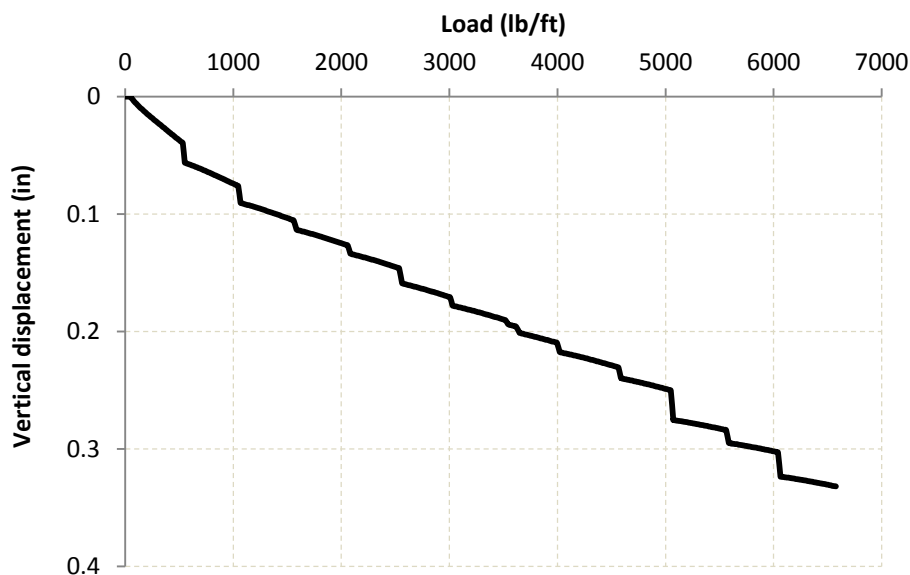
FIGURE 4.8
Vertical Displacement of the HMA Overlay versus the Applied Static Load

FIGURE 4.9
Horizontal Deformation of the HMA Overlay versus the Applied Static Load

FIGURE 4.10
Calculated Strain versus the Applied Load

51

FIGURE 4.11
Lifting of the HMA Overlay from the Edges of the Concrete Blocks

(a) Cracks on top of the HMA overlay

(b) Cracks on one side of the HMA overlay

FIGURE 4.12
Crack Lines on the HMA Overlay after the Static Loading Test

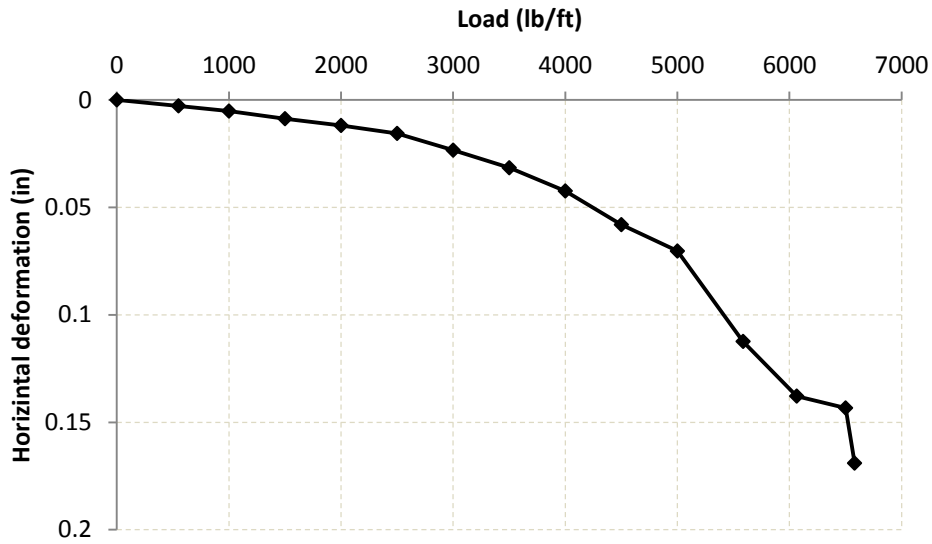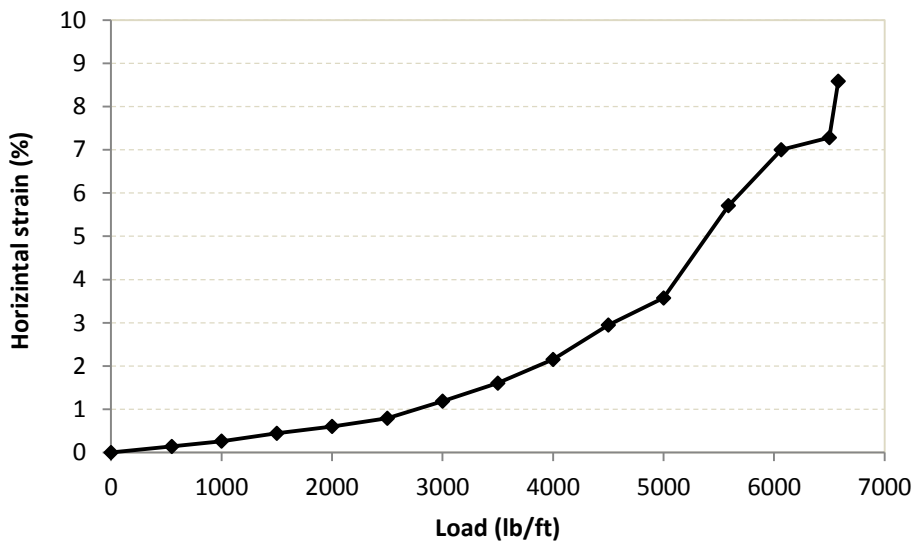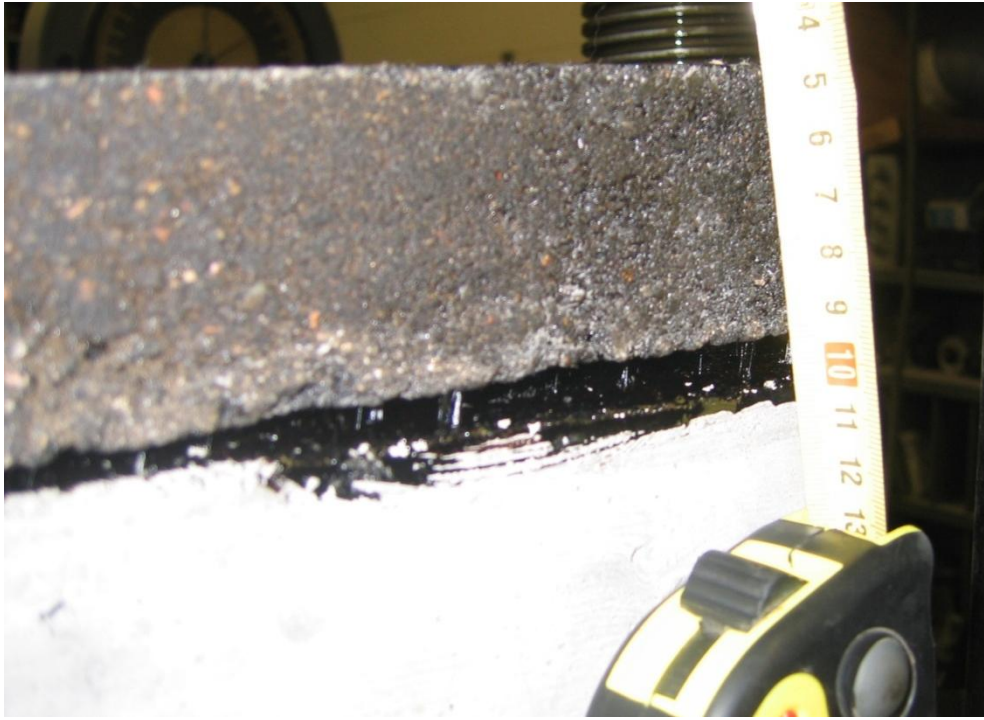Twelve cyclic loading tests were conducted on HMA overlays on two concrete blocks with gap widths of 0.2, 0.4, and 0.6 inches and subjected to three different magnitudes of loads. The cyclic loads were applied at 2,000 lb/ft, 1,500 lb/ft, and 1,000 lb/ft, respectively. During all the tests, visual observations were made at a regular interval to monitor the development of vertical cracks. Tables 4.9 and 4.10 present the test parameters and the number of loading cycles for the visually observed cracks on 1.5 and 2.0 inch thick HMA overlays over gapped concrete blocks under cyclic loading.

TABLE 4.9
Test Parameters and Visual Observations of Cracks on 1.5 Inch Thick Overlays

Sample #	1	2	3	4	5	6
	Test 1	Test 2				
Specific gravity of HMA slab	2.245	2.240	2.246	2.245	2.234	2.229
Loading frequency (Hz)	0.25	0.25	0.25	0.25	0.25	0.20
Gap between concrete blocks (inch)	0.4	0.4	0.6	0.4	0.2	0.4
Applied peak load (lb/ft)	1500	1500	1500	1000	1500	2000
First crack (hair line at the bottom side) observed at the number of cycles	135	150	105	81	50	25
Visible crack on both sides reached ¾ thickness at the number of cycles	-	-	-	-	-	-
Crack line reached the top surface at the number of cycles	1800	1500	450	4500	900	1200
Test terminated after the number of cycles	5250	5350	5150	5645	5492	5397

TABLE 4.10
Test Parameters and Visual Observations of Cracks on 2.0 Inch Thick Overlays

Sample #	1	2	3	4	5	6
	Test 1	Test 2				
Specific gravity of HMA slab	-	-	2.225	2.175	2.230	2.228
Loading frequency (Hz)	0.25	0.25	0.25	0.25	0.25	0.20
Gap between concrete blocks (inch)	0.4	0.4	0.6	0.4	0.2	0.4
Applied peak load (lb/ft)	1500	1500	1500	1000	1500	2000
First crack (hair line at the bottom side) observed at the number of cycles	700	500	150	100	300	12
Visible crack on both sides reached ¾ thickness at the number of cycles	1600	1650	450	1400	-	-
Crack line reached the top surface at the number of cycles	2700	4800	675	4500	9000	1800
Test terminated after the number of cycles	17500	10100	5050	10600	19940	5407

Different failure modes were observed during the cyclic tests: (1) bending failure with crack(s) initiated from the bottom of a specimen (Figure 4.13), (2) bending failure with crack(s) initiated from the top of a specimen (Figure 4.14), (3) shear failure with crack(s) initiated from the top of a specimen (Figure 4.15), and (4) combined bending and shear failure (Figure 4.16). Shear failure would not induce a large tensile strain on the overlay while bending failure would induce a large tensile strain on the overlay until crack(s) were formed. Since the displacement transducer was placed close to the bottom of the sample, it would measure a large strain only if the bending failure started from the bottom of the sample.
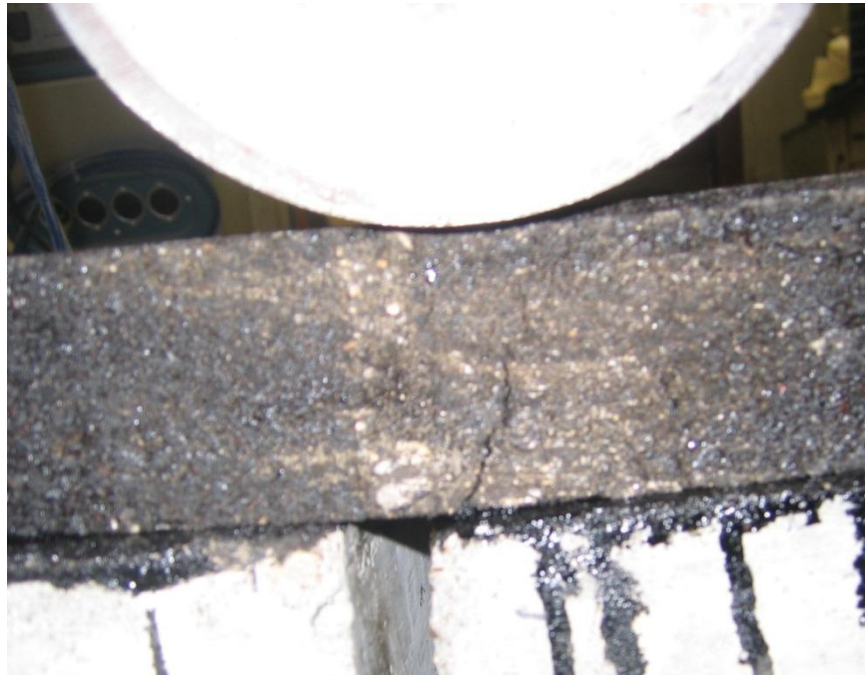
FIGURE 4.13
Crack Initiated Due to Bending from the Bottom of the HMA Overlay

FIGURE 4.14
Crack Initiated Due to Bending from the Top of the HMA Overlay

FIGURE 4.15
Crack Initiated Due to Shear from the Top of the HMA Overlay

(a) 2.0 inch overlay over a 0.4 inch wide gap

(b) 2.0 inch overlay over a 0.6 inch wide gap

FIGURE 4.16
A Combined Failure of Shear and Bending of the HMA Overlay over the Concrete Blocks with a 0.6 Inch Wide Gap

4.2 Discussions

4.2.1 Direct Shear Box Tests

Load-displacement curves obtained from the direct shear box tests were used to determine the shear displacements of the HMA specimens at the maximum loads. Prior to such determination, each load-displacement curve was corrected for the initial portion of the curve. Because of a seating error between an HMA specimen and concrete blocks, the initial portion of the load-displacement curve does not necessarily give an accurate response of the HMA specimen as shown in Figure 4.17(a). To correct this error, the whole load-displacement curve should be shifted towards the origin by a certain amount of offset. The required offset was determined by drawing a straight line on the linear portion of the load-displacement curve to intercept the horizontal displacement axis. Figures 4.17(b) and (c) show the detailed steps to correct a typical load-displacement curve obtained from a direct shear box test. Once the load-displacement curve was corrected, the shear displacement at the maximum load was determined. Tables 4.11 to 4.14 show the shear displacements at their corresponding maximum loads for all the HMA specimens tested.
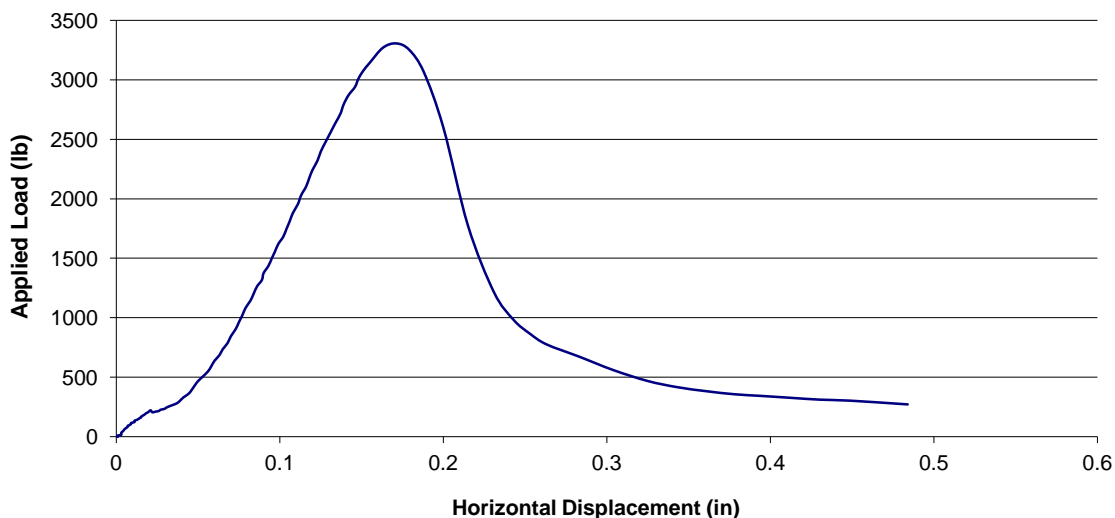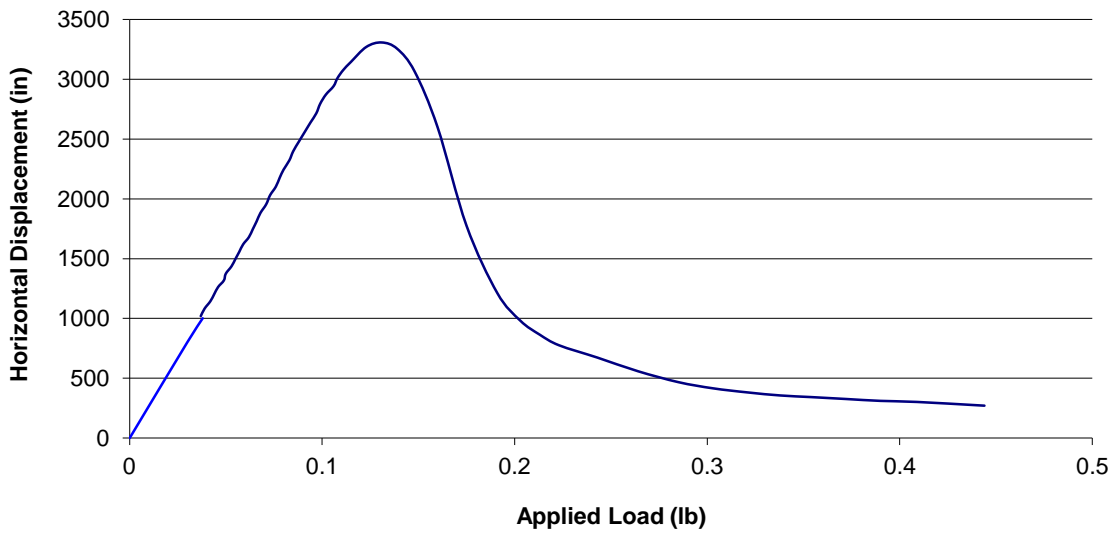

(a) An uncorrected load-displacement curve

FIGURE 4.17
Correction of a Load-Displacement Curve from a Direct Shear Box Test

59
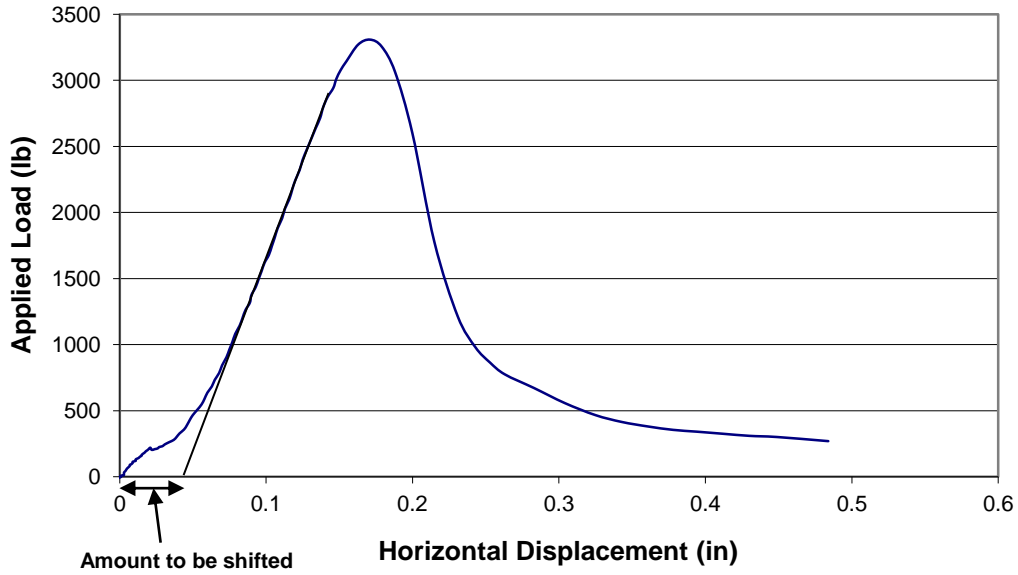
(b) Determination of the offset to be shifted

Applied Load Vs Horizontal Displacement

(c) Corrected load-displacement curve

FIGURE 4.17
Correction of a Load-Displacement Curve from a Direct Shear Box Test

TABLE 4.11
Displacements at the Maximum Loads for 1.5 Inch Mix 1 Specimens

Specimen #	Gap Width (inch)	Bulk Specific Gravity	Maximum Load (lb)	Shear Displacement (inch)
1	0.5	2.214	1117	0.110
2	0.5	2.199	897	0.131
3	0.5	2.199	1092	0.141
4	0.375	2.221	1194	0.133
5	0.375	2.230	1161	0.119
6	0.375	2.251	1353	0.108
7	0.25	2.143	852	0.117
8	0.25	2.191	928	0.099
9	0.25	2.180	989	0.097

TABLE 4.12
Displacements at the Maximum Loads for 2.0 Inch Mix 1 Specimens

Specimen #	Gap Width (inch)	Bulk Specific Gravity	Maximum Load (lb)	Shear Displacement (inch)
1	0.5	2.285	1829	0.137
2	0.5	2.265	1825	0.119
3	0.5	2.230	1385	0.139
4	0.375	2.245	1774	0.118
5	0.375	2.244	1366	0.126
6	0.375	2.257	1536	0.126
7	0.25	2.196	1100	0.141
8	0.25	2.191	1633	0.096
9	0.25	2.223	1421	0.138

TABLE 4.13
Displacements at the Maximum Loads for 1.5 Inch Mix 2 Specimens

Specimen #	Gap Width (inch)	Bulk Specific Gravity	Maximum Load (lb)	Shear Displacement (inch)
1	0.5	2.263	2511	0.106
2	0.5	2.306	2333	0.107
3	0.5	2.294	2412	0.106
4	0.375	2.310	2305	0.116
5	0.375	2.303	2484	0.081
6	0.375	2.301	2368	0.102
7	0.25	2.291	2816	0.092
8	0.25	2.264	2131	0.097
9	0.25	2.278	2696	0.116

TABLE 4.14
Displacements at the Maximum Loads for 2.0 Inch Mix 2 Specimens

Specimen #	Gap Width (inch)	Bulk Specific Gravity	Maximum Load (lb)	Shear Displacement (inch)
1	0.5	2.377	3073	0.136
2	0.5	2.365	3385	0.110
3	0.5	2.356	3347	0.091
4	0.375	2.370	3371	0.118
5	0.375	2.366	3188	0.121
6	0.375	2.316	3211	0.11
7	0.25	2.323	3100	0.12
8	0.25	2.340	3135	0.091
9	0.25	2.340	3307	0.111

Figures 4.18 and 4.19 show the averaged maximum shear load versus the gap width. It is shown that the maximum shear load did not vary much with the gap width. The thicker (2.0 inch) specimens had higher maximum shear loads than the thinner (1.5 inch) specimens. In addition, the Mix 2 specimens had approximately double maximum shear loads as the Mix 1 specimens because the stiffer asphalt binder was used in Mix 2.
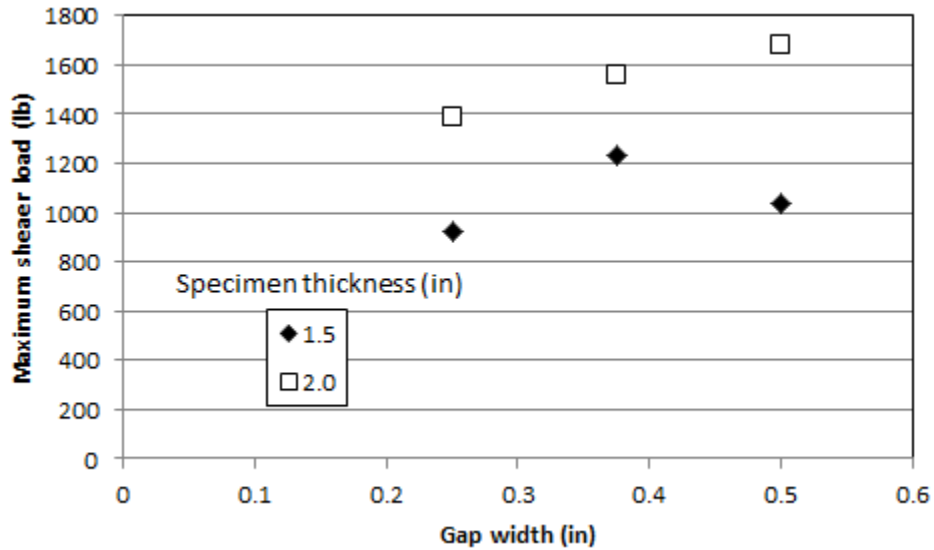

FIGURE 4.18
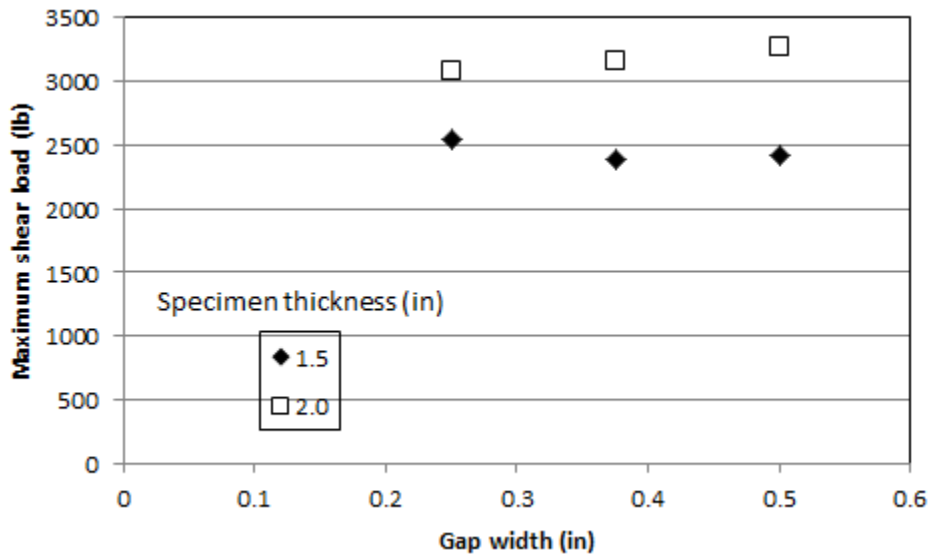**Maximum Shear Load versus Gap Width for Mix 1**

FIGURE 4.19
Maximum Shear Load versus Gap Width for Mix 2

Figures 4.20 and 4.21 show the corresponding averaged displacement at the maximum load versus the gap width. It can be seen that there was a minor effect of the gap width on the displacement at a maximum load**.** The displacements corresponding to the maximum loads ranged from 0.10 to 0.14 inches and the Mix 2 specimens had slightly smaller shear displacements than the Mix 1 specimens due to the same reason as the maximum shear load (i.e., Mix 2 had stiffer asphalt binder). Figure 4.22 shows that the shear displacement at the maximum load varied between 6.0 to 9.0% of the specimen thickness with an average of 7.7%.
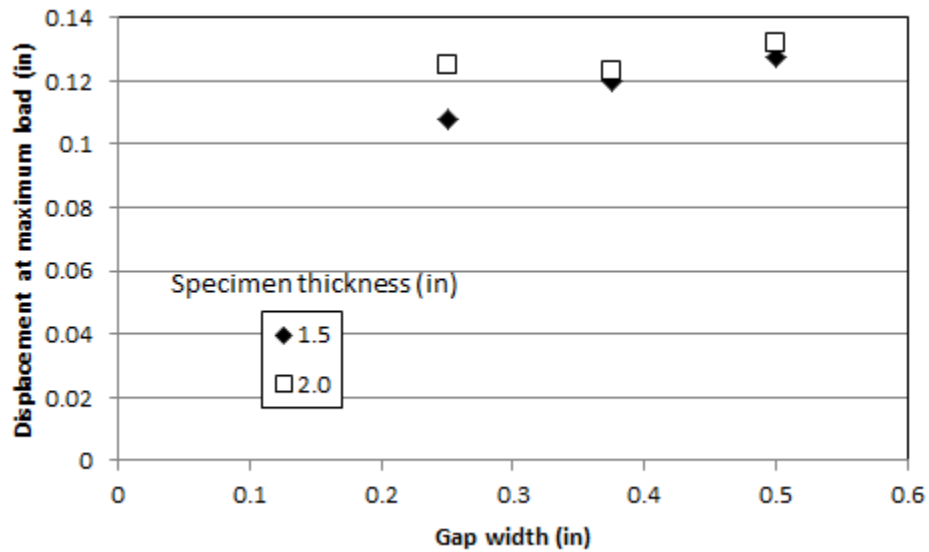

FIGURE 4.20
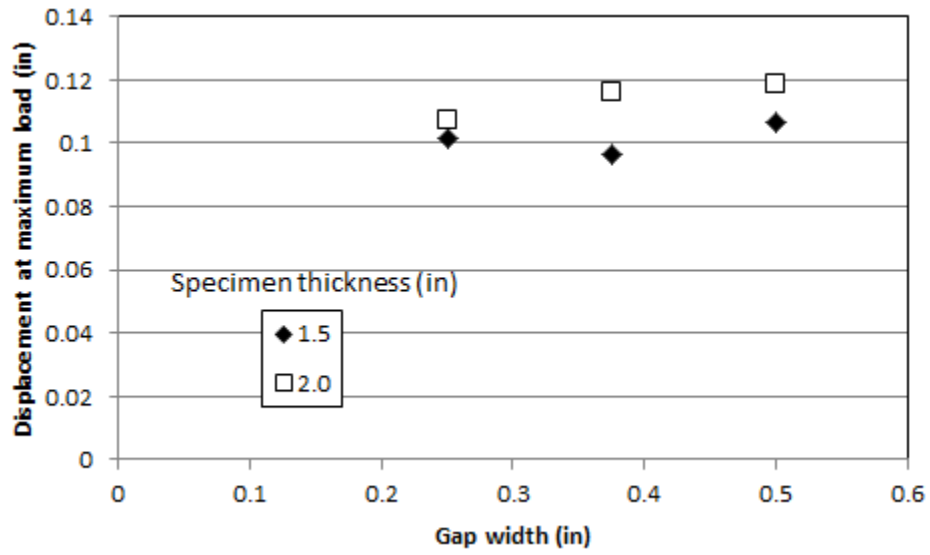**Effect of the Gap Width on the Displacement at the Maximum Load for Mix 1**

FIGURE 4.21
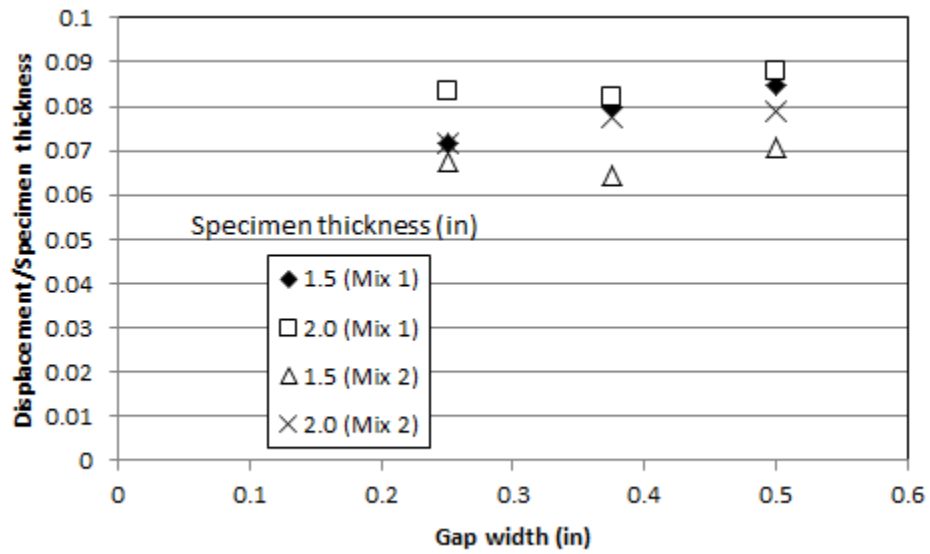**Effect of the Gap Width on the Displacement at the Maximum Load for Mix 2**

FIGURE 4.22
Ratio of Shear Displacement to Specimen Thickness versus Gap Width

4.2.2 Semi-Circular Bend Tests

Figures 4.23 and 4.24 present the number of cycles before failure of specimens for both Mix 1 and Mix 2 at different levels of loading as compared with the maximum static loads from the static semi-circular bend tests. It is shown that an increase of the percentage of the maximum static load reduced the number of cycles to failure. For Mix 1, 2.0 inch thick specimens had a higher number of cycles than 1.5 inch thick specimens. For Mix 2, however, their difference is undistinguishable.
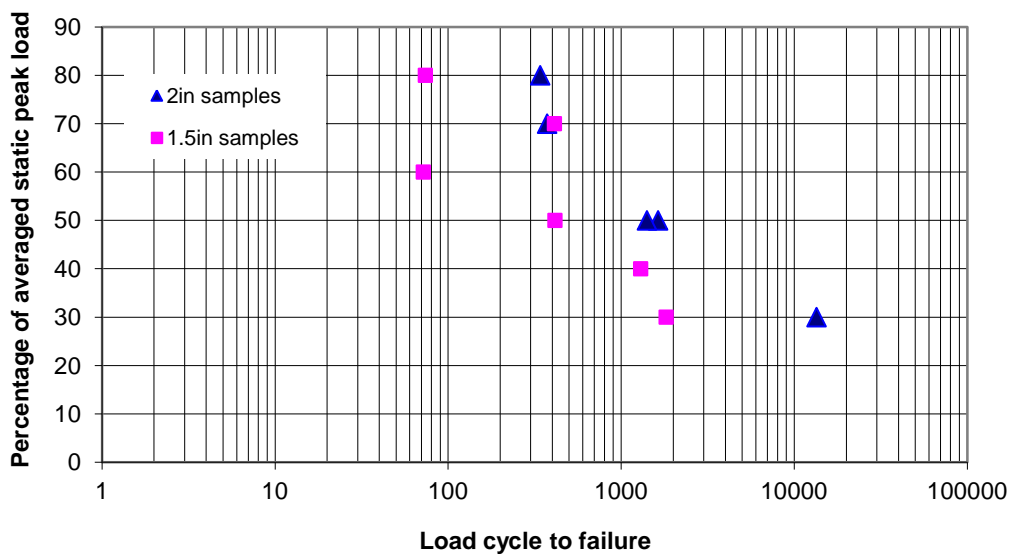

FIGURE 4.23
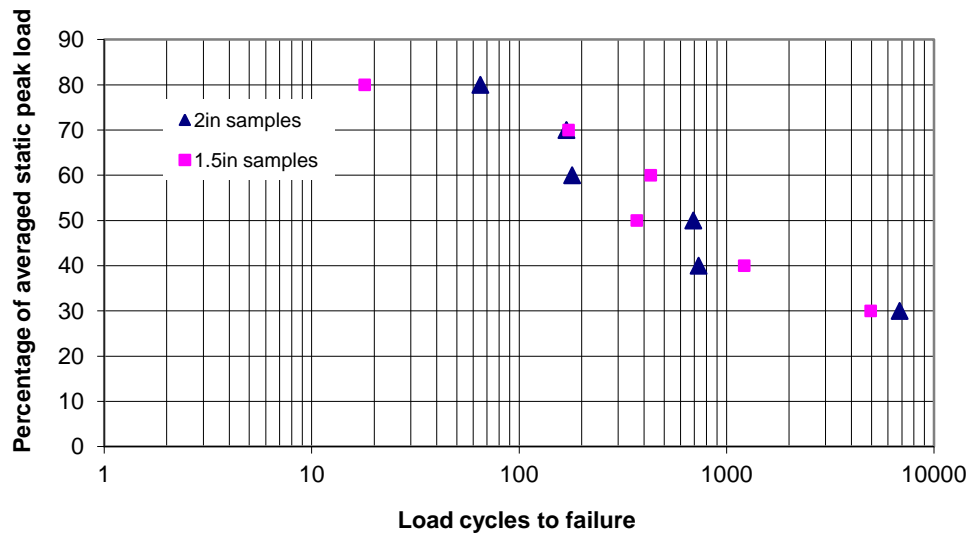**Cyclic Load at the Percentage of the Averaged Static Maximum Load versus the Number of Load Cycles to Failure for Mix 1**

FIGURE 4.24
Cyclic Load at the Percentage of Averaged Static Maximum Load
versus the Number of Load Cycles to Failure for Mix 2

Tolerable strain (defined as the strain at the initial crack) is determined by the intersection of two straight lines drawn on the linear portion of the strain versus load cycle curve in a cyclic semi-circular bend test. Figure 4.25 shows the systematic way of determining a tolerable strain of an HMA specimen. Table 4.15 shows the comparison between the visually observed and calculated load cycles to failure, which are in good agreement.

Figures 4.26 and 4.27 show the relationship between the number of cycles to the initial crack of the HMA specimen and the static strain at the same load level. In general, the number of cycles to the initial crack decreased with an increase in the static strain in the HMA sample except the 2.0 inch specimens for Mix 1.

TABLE 4.15
Observed and Calculated Load Cycles to the Initial Crack

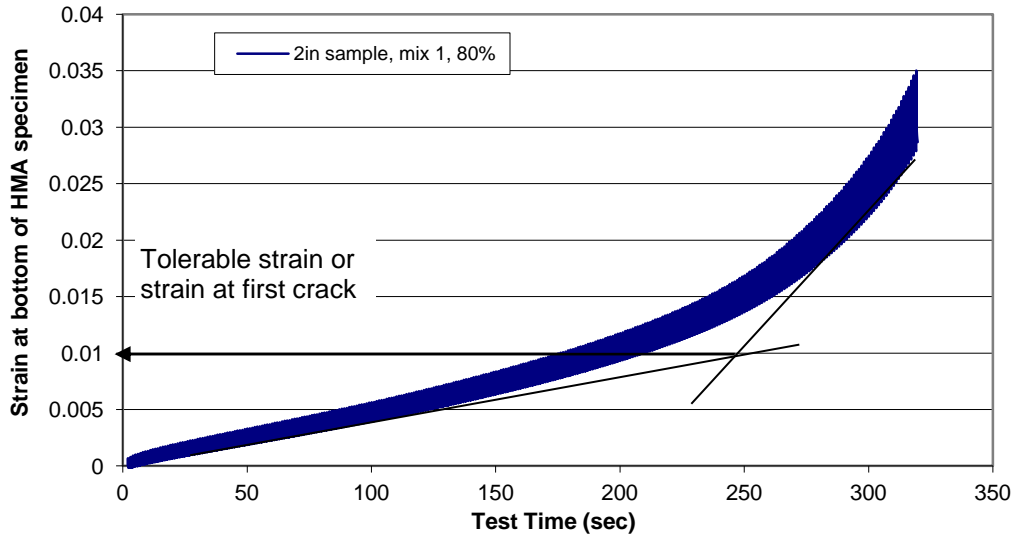| Mix Type	Percentage of maximum static load (%)	Thickness (inch)	Observed load cycles to the initial crack	Calculated load cycles to the initial crack
1	70	1.5	220	210
1	60	1.5	37	34
1	50	1.5	224	240
1	40	1.5	818	802
1	30	1.5	820	818
1	80	2	296	265
1	70	2	330	215
1	50	2	1258	1133
1	30	2	11170	11095
2	80	1.5	10	10
2	70	1.5	175	173
2	60	1.5	695	431
2	50	1.5	355	369
2	40	1.5	968	1216
2	30	1.5	3848	4951
2	80	2	63	51
2	70	2	140	129
2	60	2	150	165
2	50	2	645	673
2	40	2	673	673
2	30	2	6274	6827

FIGURE 4.25
Systematic Way of Determining the Tolerable Strain for an HMA
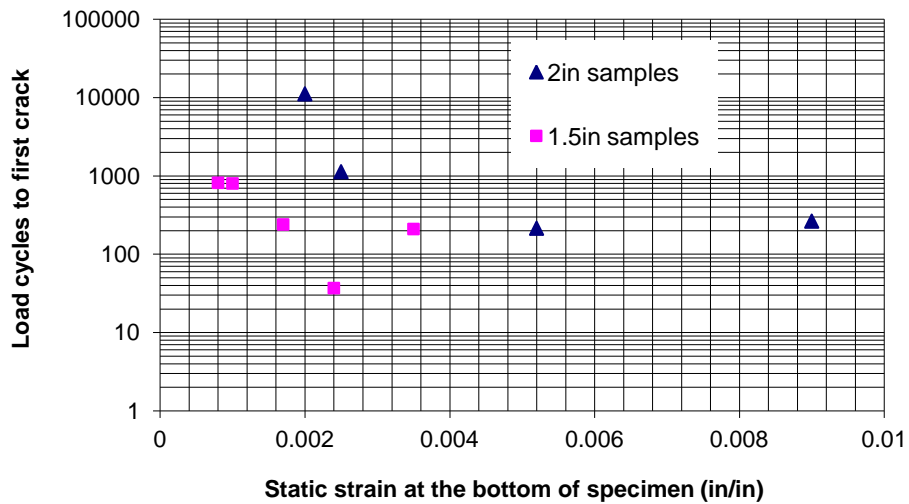**Mixture**

FIGURE 4.26
Number of Load Cycles to the Initial Crack versus the Static
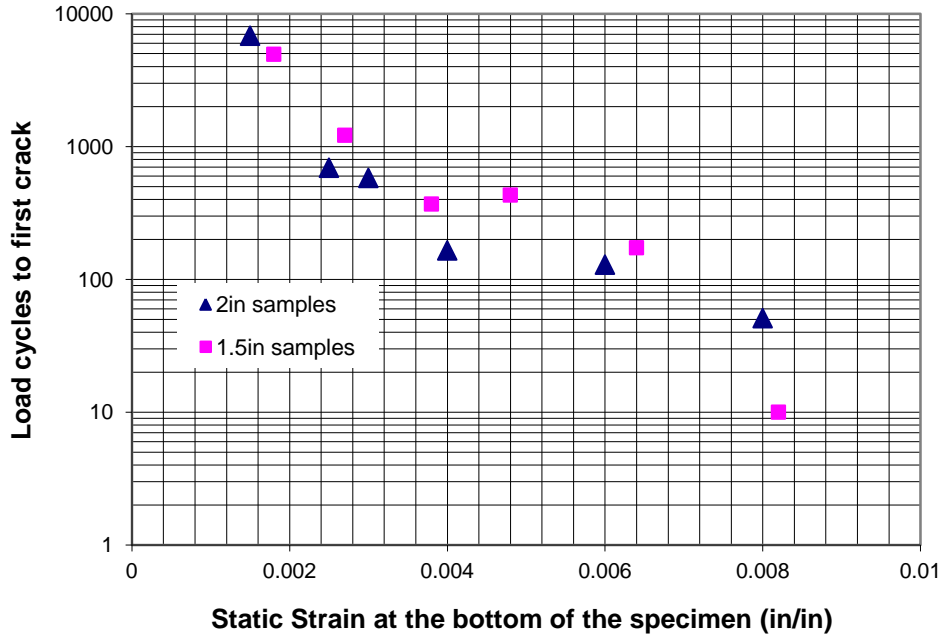**Strain at the Bottom of the HMA Specimen for Mix 1**

71

FIGURE 4.27
Number of Load Cycles to the Initial Crack versus the Static
Strain at the Bottom of the HMA Specimen for Mix 2

Figures 4.28 and 4.29 show the relationship between the static and cyclic permanent strains developing at the bottom of the specimen when the initial crack occurred. The strain at the bottom of the specimen when the initial crack occurred is referred as the tolerable strain. It is shown that the tolerable strain under cyclic loading decreased with an increase of the static strain in the specimen under the same level of static loading. The level of the tolerable strain under cyclic loading was mostly higher than that under static loading. The Mix 2 specimens had lower tolerable tensile strains under cyclic loading than the Mix 1 specimens because Mix 2 used more brittle asphalt binder.
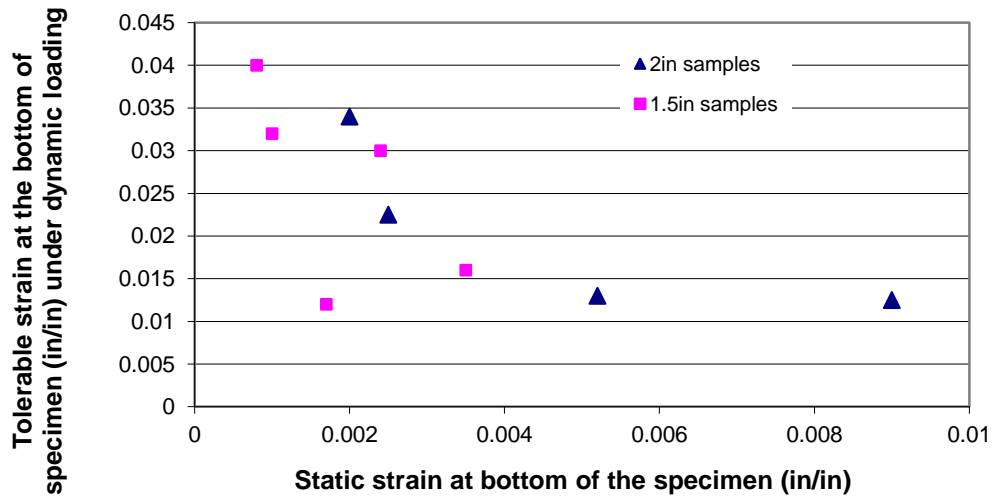
FIGURE 4.28
Tolerable Strain under Cyclic Loading versus the Static Strain at the
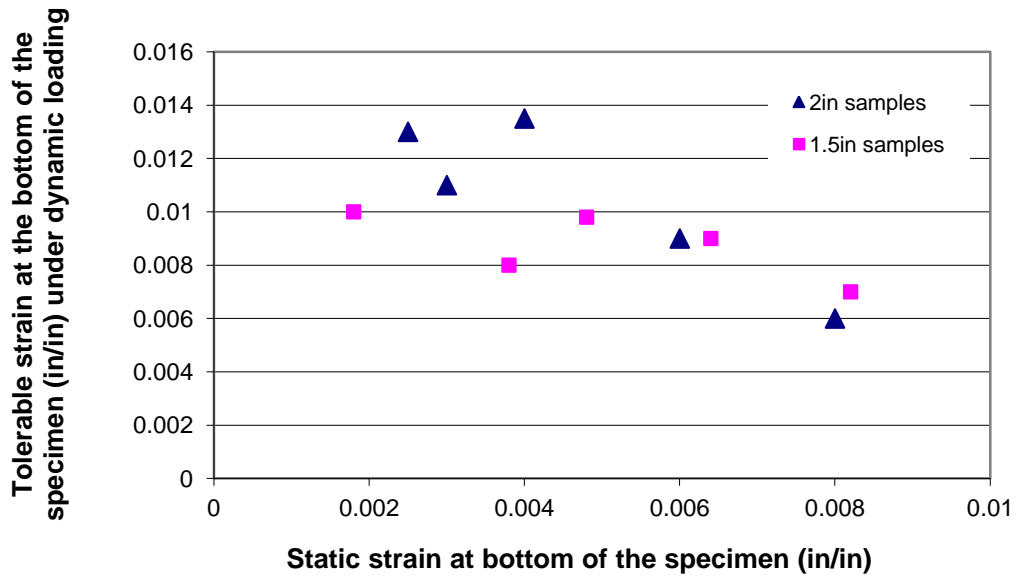**Bottom of the Specimen for Mix 1**

FIGURE 4.29
Tolerable Strain under Cyclic Loading versus the Static Strain at the
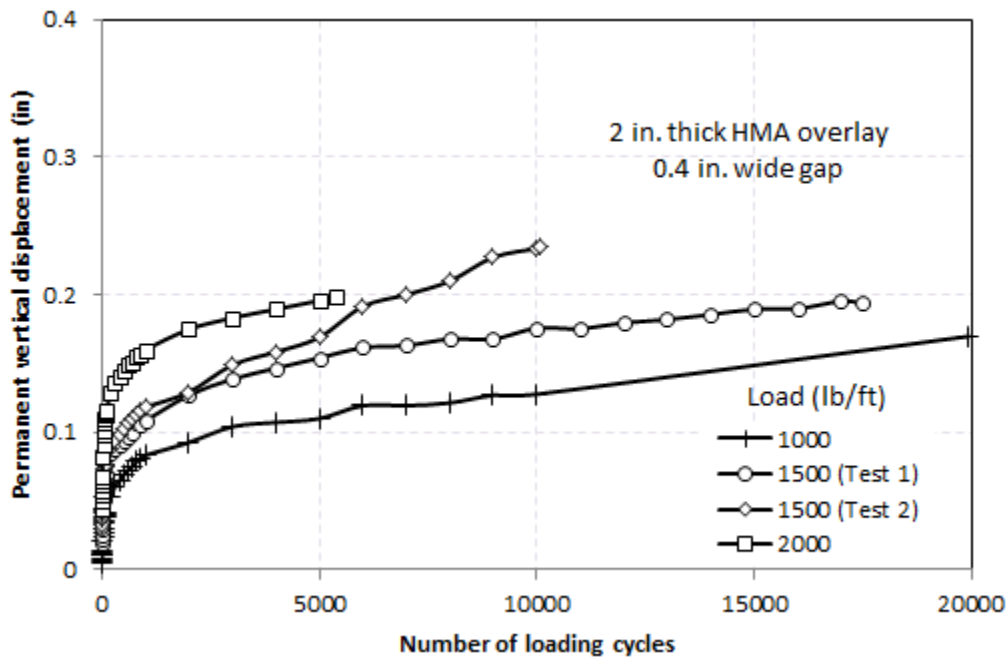**Bottom of the Specimen for Mix 2**

4.2.3 HMA Overlay Loading Tests

Figure 4.30 presents the development of the permanent vertical displacement with the number of loading cycles for the 1.5 inch or 2.0 inch thick HMA overlay over concrete blocks with a 0.4 inch wide gap under different loading magnitude. The permanent vertical displacement increased rapidly within the initial few cycles and continued increasing at a slower rate. Two tests (Tests 1 and 2) done at the same load and gap width for each HMA overlay thickness (1.5 or 2.0 inch) show reasonable repeatability of the test method (the difference in the later stage of the tests for the 2.0 inch thick specimens is not important because the specimens had failed after 4,800 cycles). Test results also show that the increase of the applied load increased the permanent vertical displacement of the HMA overlay. The thicker (2.0 inch) specimen had a smaller displacement than the thinner (1.5 inch) specimen.

Figure 4.31 presents the development of the permanent vertical displacement with the number of loading cycles for the 1.5 inch or 2 inch thick HMA overlay over concrete blocks with different gap width under the same loading magnitude of 1,500 lb/ft. Again, the test results show good repeatability of the test method. In general, the increase of the gap width increased the permanent vertical displacement of the HMA overlay.
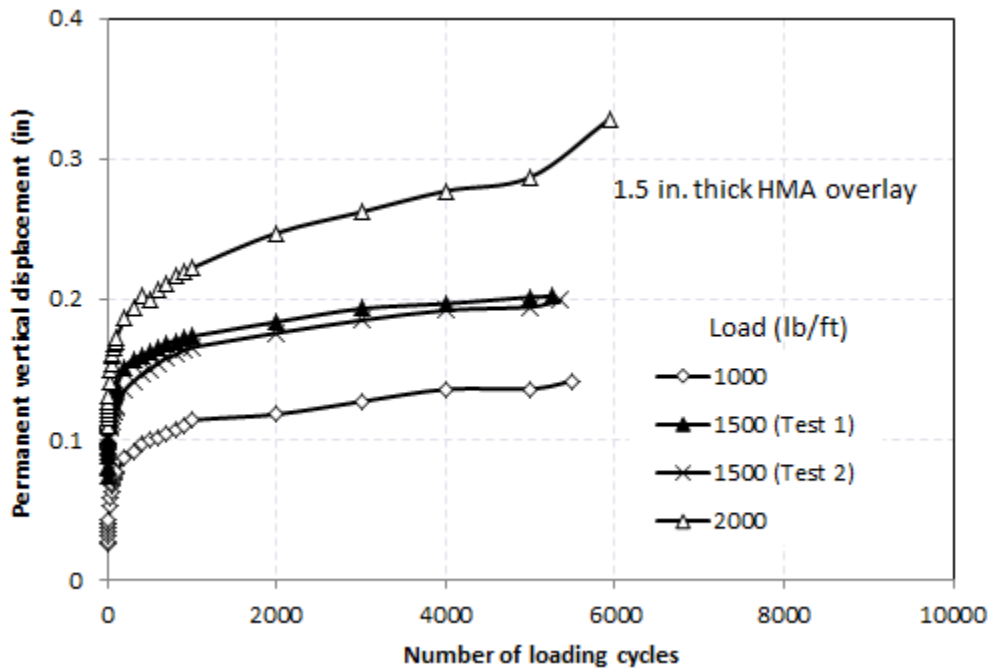
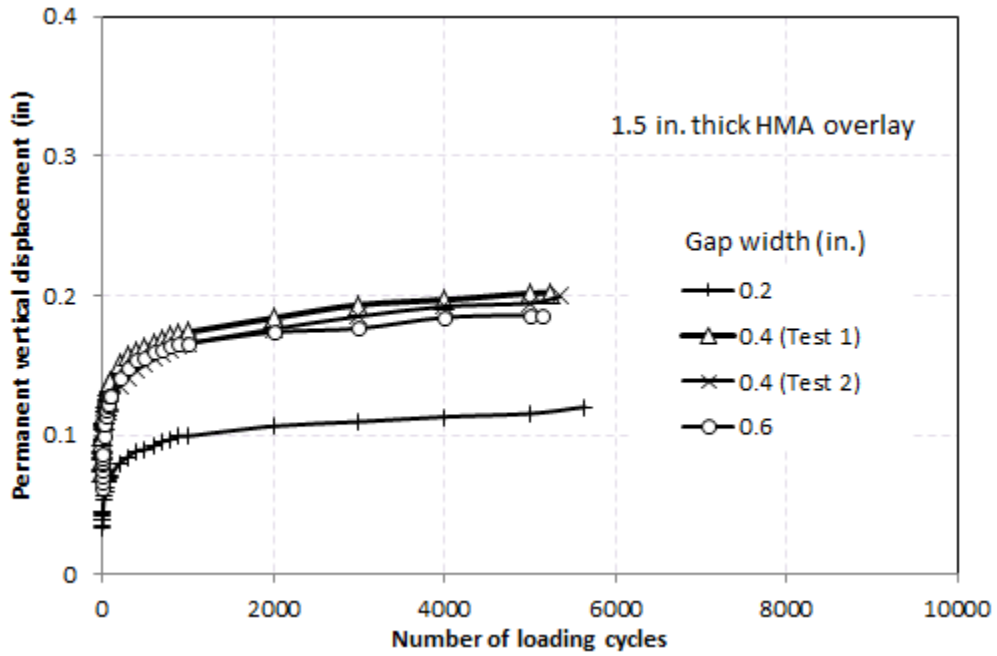(a) 1.5 inch thick HMA overlay

(b) 2.0 inch thick HMA overlay

FIGURE 4.30
Permanent Vertical Displacement of the HMA Overlay versus the Number of Loading Cycles over Concrete Blocks with a 0.4 Inch Wide Gap at Different Loading Magnitude

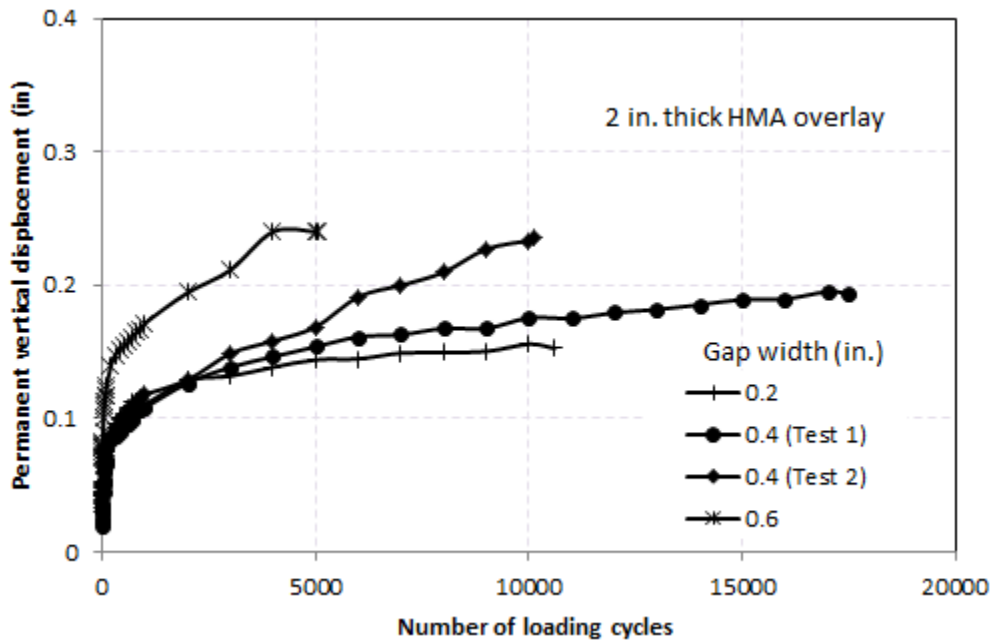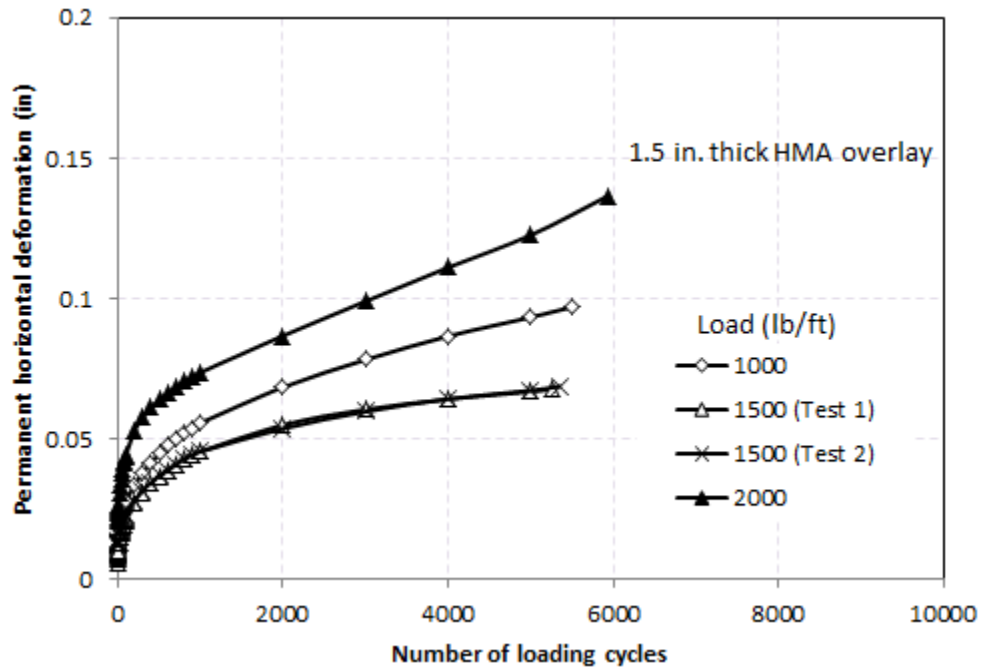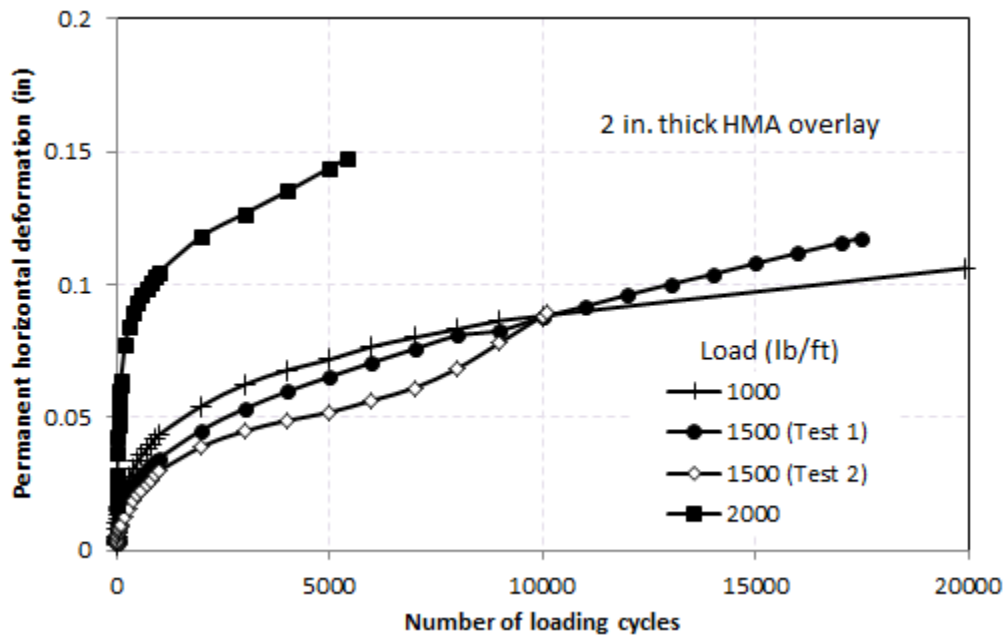(a) 1.5 inch thick HMA overlay

(b) 2.0 inch thick HMA overlay

FIGURE 4.31
Permanent Vertical Deformation of the HMA Overlay versus the
Number of Loading Cycles over Concrete Blocks with Different
Gap Width at a Load of 1,500 lb/ft

Figure 4.32 presents the development of the permanent horizontal deformation with the number of loading cycles for the 1.5 inch or 2.0 inch thick HMA overlay over concrete blocks with a 0.4 inch wide gap under different loading magnitude. Similar to the permanent vertical displacement, the permanent horizontal deformation increased with the number of loading cycles. However, the effect of the applied load on the permanent horizontal deformation is different from that on the permanent vertical deformation. It is interesting to notice that the permanent horizontal deformation for the overlay under the load of 1,000 lb/ft was larger than that under the load of 1,500 lb/ft. The possible explanation is that under the load of 1,000 lb/ft, the overlay was mostly subjected to a bending failure, which induced a larger permanent horizontal deformation, while under the load of 1,500 lb/ft, the overlay was mostly subjected to a shear failure, which induced a smaller permanent horizontal deformation.

(a) 1.5 inch thick HMA overlay

(b) 2.0 inch thick HMA overlay

FIGURE 4.32
Permanent Horizontal Deformation of the HMA Overlay versus the Number of Loading Cycles over Concrete Blocks with a 0.4 Inch Wide Gap at Different Loading Magnitude

Figure 4.33 presents the development of the permanent horizontal deformation with the number of loading cycles for the 1.5 inch or 2.0 inch thick HMA overlay over concrete blocks with different gap width under the same loading magnitude of 1,500 lb/ft. It is clearly shown that the wider gap induced more permanent horizontal deformation. This result implies that a wider gap promotes a bending failure. The direct shear test results discussed earlier show that the increase of the gap width did not change the shear capacity much.
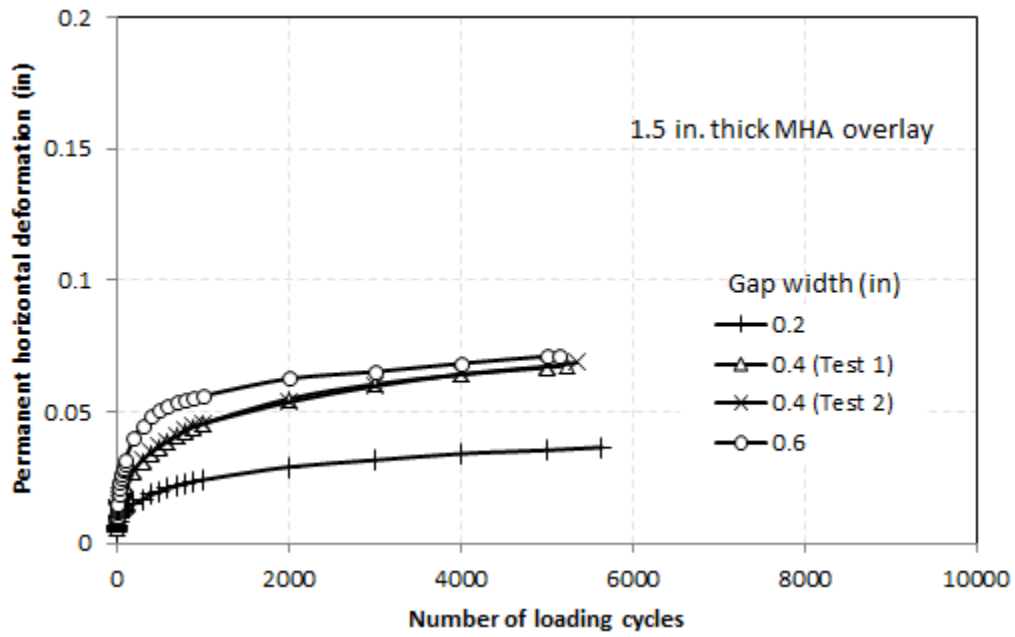
(a) 1.5 inch thick HMA overlay
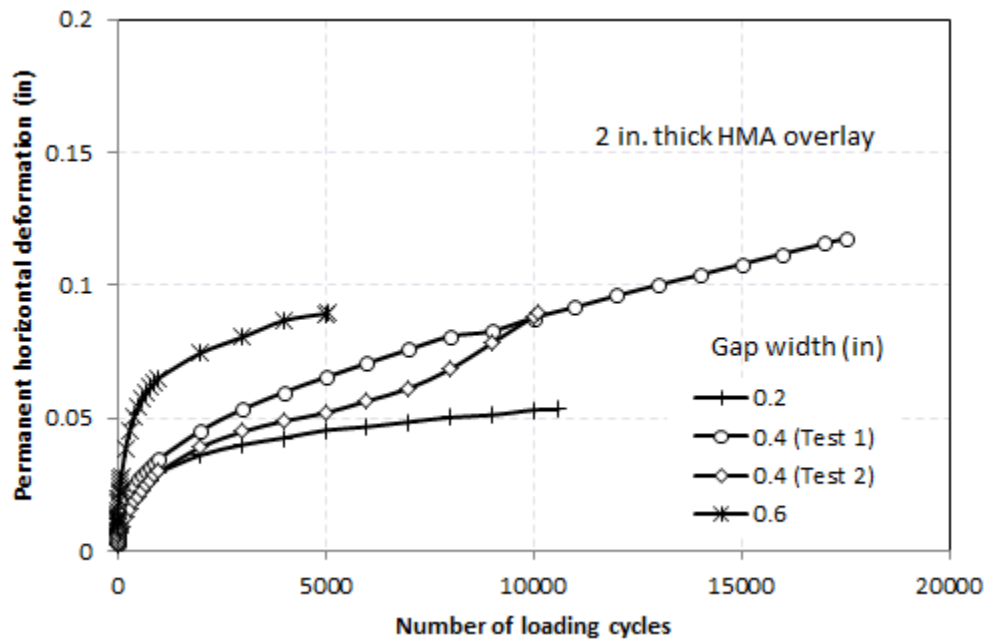
(b) 2.0 inch thick HMA overlay

FIGURE 4.33
Permanent Horizontal Deformation of the HMA Overlay over a Gap of Different Width versus the Number of Loading Cycles at 1,500 lb/ft

Tables 4.16 and 4.17 summarize the permanent horizontal deformations and vertical displacements at the initial crack and failure of the 1.5 or 2.0 inch thick HMA overlay under cyclic loading. The failure of the overlay is defined as the crack propagated to the top surface. The number of loading cycles required to fail the overlay is presented in Figure 4.34, which shows the thicker (2 inch) overlay had a larger number of loading cycles than the thinner (1.5 inch) overlay. The increase of the applied load or gap width reduced the number of loading cycles. The number of loading cycles and other performance parameters (to be presented later) at the load of 1,500 lb/ft are averaged from two tests.

TABLE 4.16
Permanent Horizontal Deformations and Vertical Displacements at the Initial Crack and Failure of the 1.5 Inch Thick HMA Overlay

Specimen #1		1	2	3	4	5	6
Permanent vertical displacement (inch)	At initial crack	0.146	0.134	0.132	0.071	0.063	0.146
	At failure	0.181	0.173	0.157	0.138	0.098	0.232
Permanent horizontal deformation (inch)	At initial crack	0.0236	0.0248	0.0315	0.0256	0.0110	0.0323
	At failure	0.0532	0.0512	0.0492	0.0886	0.0236	0.0787

TABLE 4.17
Permanent Horizontal Deformations and Vertical Displacements at the Initial Crack and Failure of the 2.0 Inch Thick HMA Overlay

Sample #1		1	2	3	4	5	6
Permanent vertical displacement (inch)	At initial crack	0.098	0.102	0.154	0.041	0.093	0.075
	At failure	0.134	0.169	0.161	0.110	0.150	0.173
Permanent horizontal deformation (inch)	At initial crack	0.0295	0.0205	0.0354	0.0181	0.0224	0.0303
	At failure	0.0512	0.0512	0.0591	0.0689	0.0504	0.1142

Figures 4.35 and 4.36 present the effects of the applied load, gap width, and overlay thickness on the permanent vertical displacements at the initial crack and failure, respectively. In general, the permanent vertical displacement increased with the applied load and gap width. The effect of the overlay thickness is inconclusive.
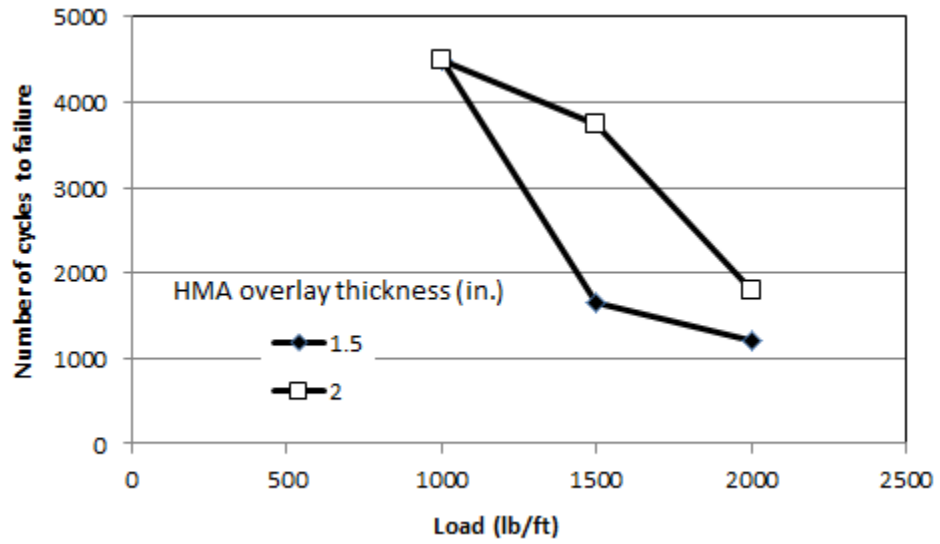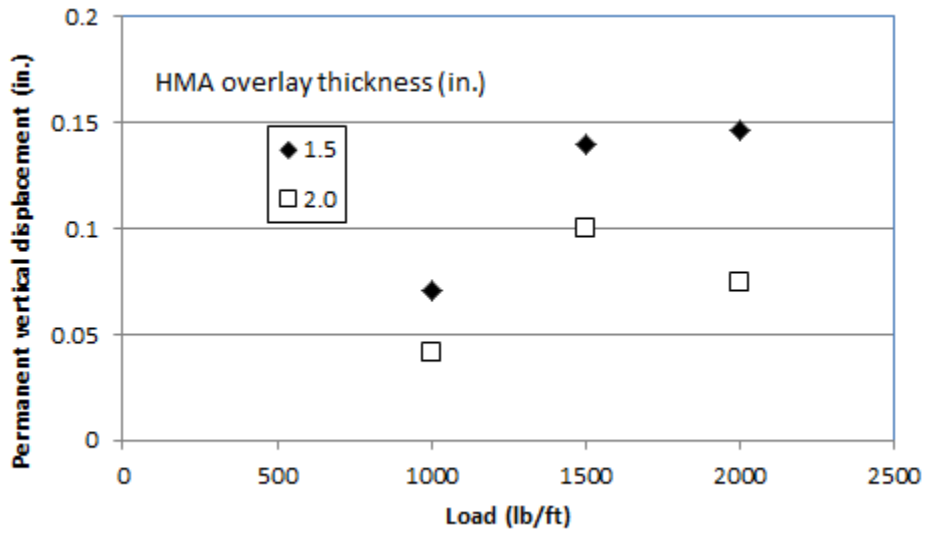
(a) Gap width = 0.4 inch
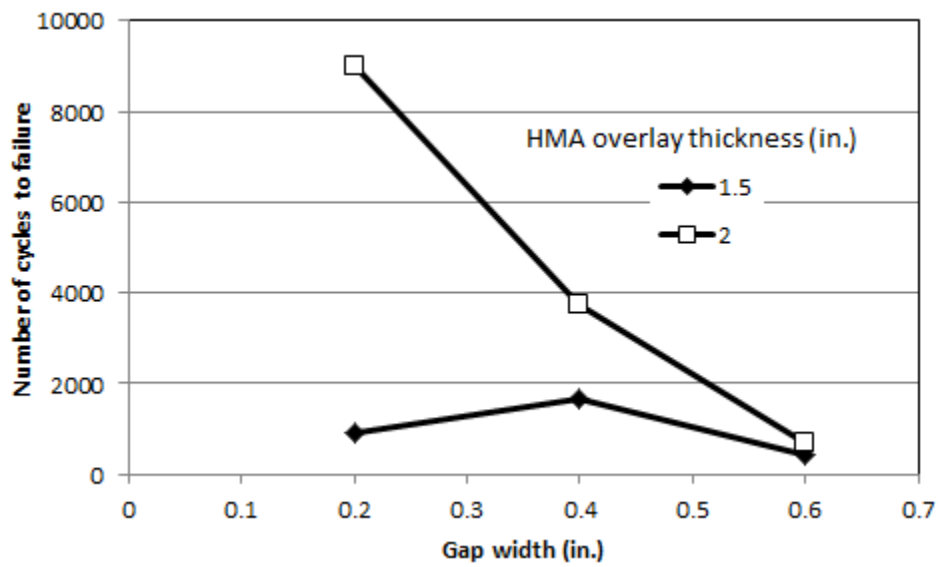
(b) Load = 1500 lb/ft

FIGURE 4.34
Number of Loading Cycles Required for the Failure of the HMA
Overlay Cyclic Loading

(a) Gap width = 0.4 inch
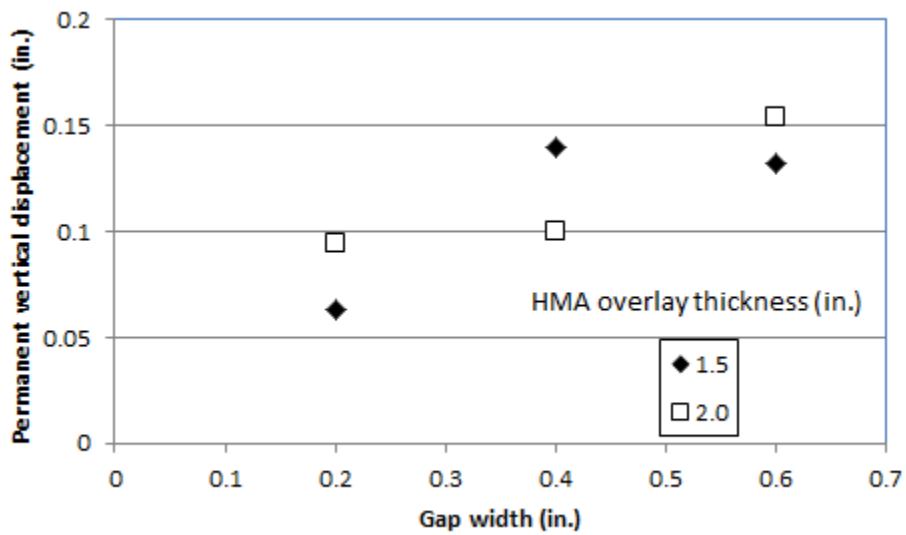
(b) Load = 1500 lb/ft

FIGURE 4.35
Permanent Vertical Displacement of HMA Overlay at the Initial Crack

84
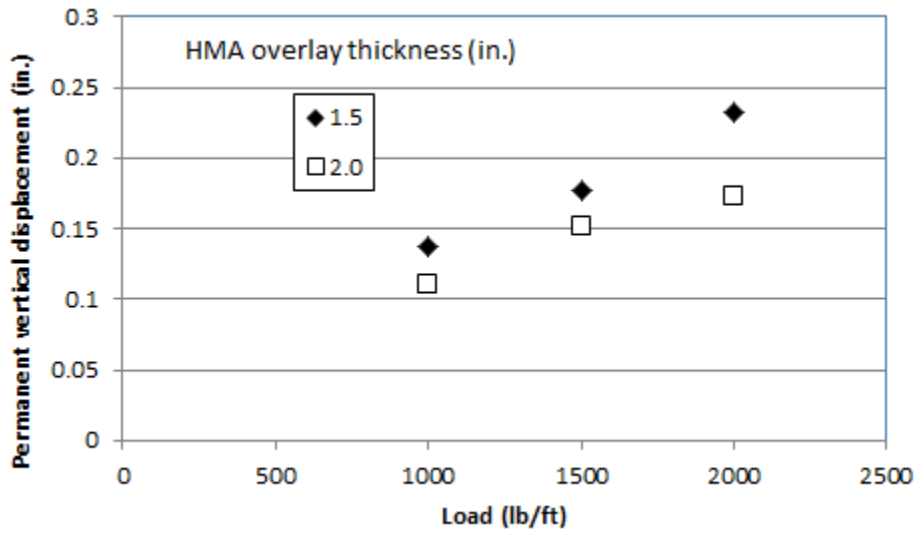
(a) Gap width = 0.4 inch
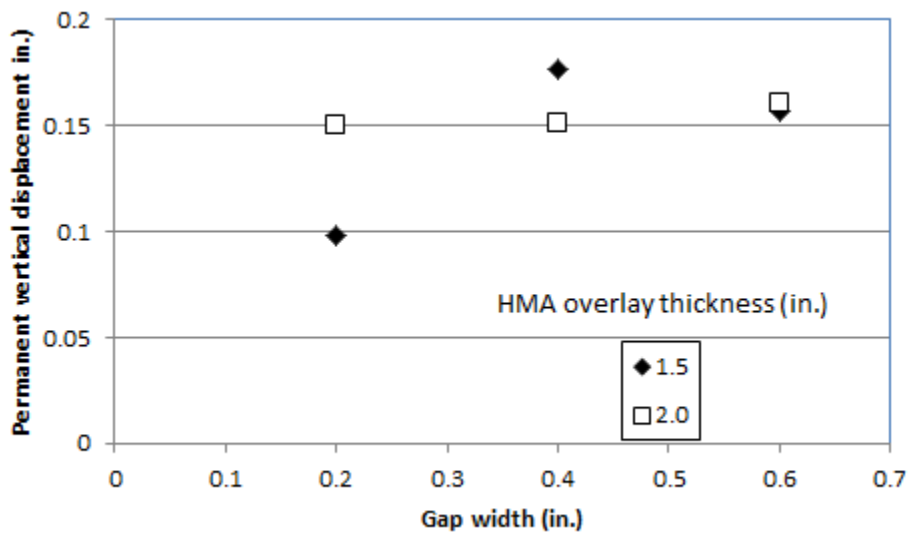
(b) Load = 1500 lb/ft

FIGURE 4.36
Permanent Vertical Displacement of HMA Overlay at Failure

Based on the measured horizontal deformation at the bottom of the HMA overlay, the average permanent tensile strain was calculated by dividing the deformation by the gauge length. The calculated average tensile strain is meaningful until the initiation of a crack and also defined

as the tolerable tensile strain of the HMA overlay. The calculated average permanent tensile strain of each 1.5 or 2.0 inch thick HMA overlay at the initial crack is reported in Table 4.18.

TABLE 4.18
Average Permanent Tensile Strain at the Initial Crack

Specimen #	1	2	3	4	5	6
1.5 inch thick HMA overlay (%)	1.18	1.24	1.58	1.28	0.55	1.62
2.0 inch thick HMA overlay (%)	1.48	1.03	1.77	0.91	1.12	1.52

Figure 4.37 presents the effects of the applied load, gap width, and overlay thickness on the tolerable tensile strain of the HMA overlay. In general, the 1.5 and 2.0 inch overlays had similar tensile strains except those at the load of 1,000 lb/ft. The tensile strains increased with the applied load and gap width.
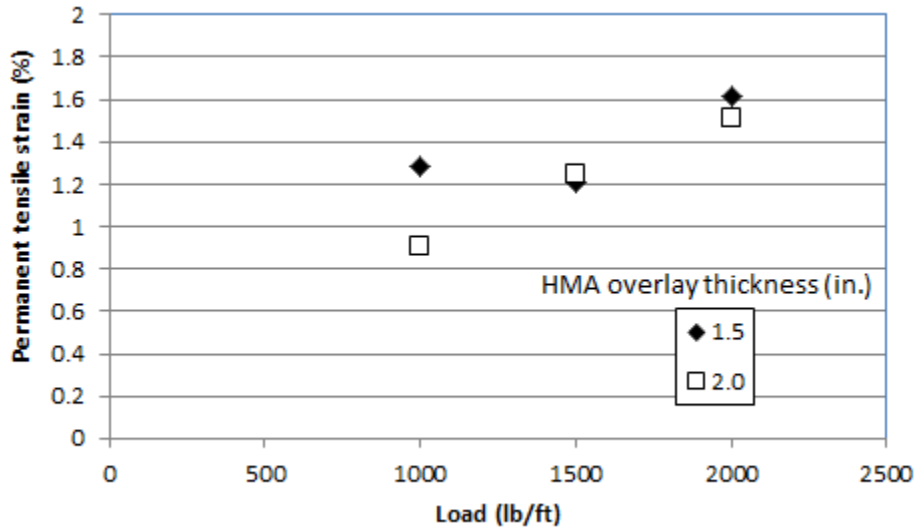
(a) Gap width = 0.4 in.
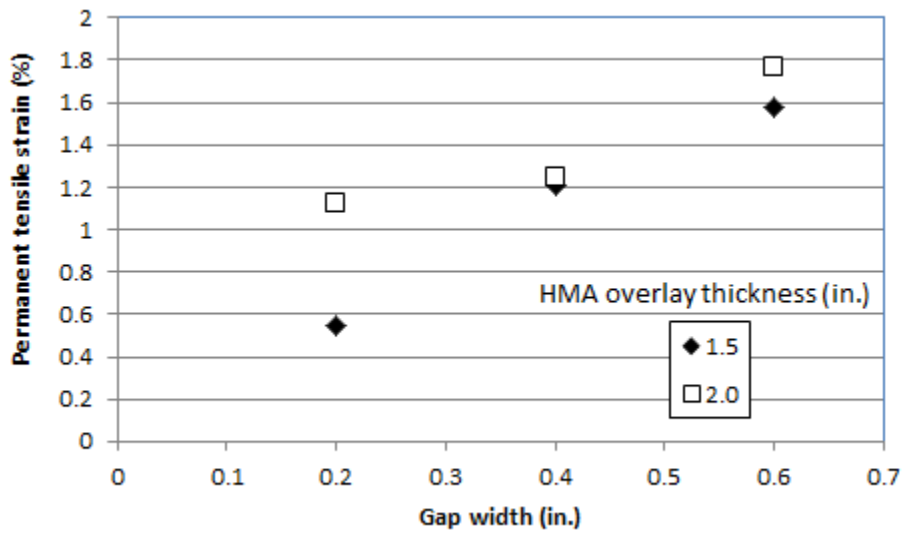
(b) Load = 1,500 lb/ft

FIGURE 4.37
Average Permanent Tensile Strain of the HMA Overlay at the
Initial Crack

Figure 4.38 presents the test results of the permanent horizontal deformation versus the applied load or gap width for the 1.5 or 2.0 inch HMA overlay at failure. In general, the permanent horizontal deformation was not sensitive to the applied load or gap width.
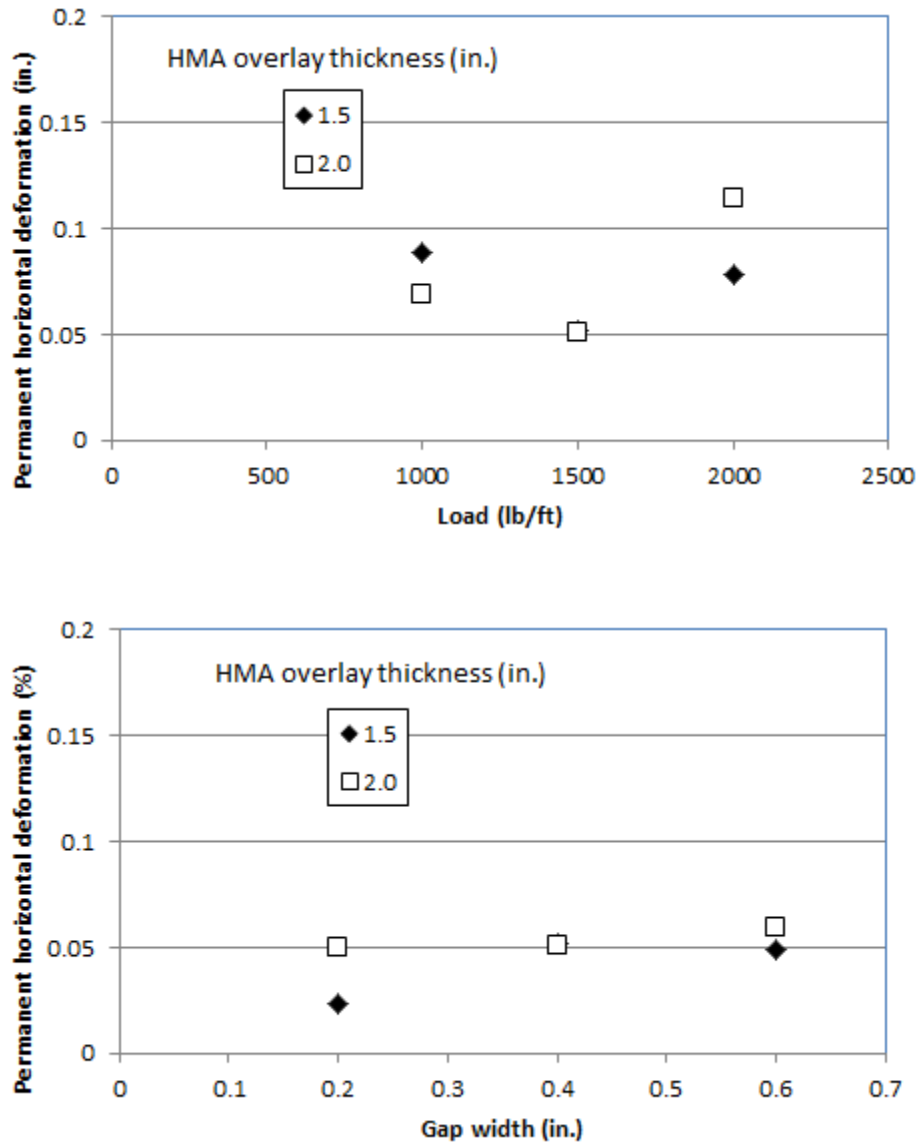
FIGURE 4.38
Permanent Horizontal Deformation of HMA Overlay at Failure

4.3 Comparison of Test Results

4.3.1 Direct Shear Test versus Semi-Circular Bend Test

Figure 4.39 shows the correlation between the peak compressive load from the static semi-circular bend test and the maximum shear load from the direct shear box test. It is shown that the maximum compressive load of the HMA sample obtained from the SCB test is approximately 1.23 times of the maximum shear load of the HMA sample obtained from the direct shear box test.
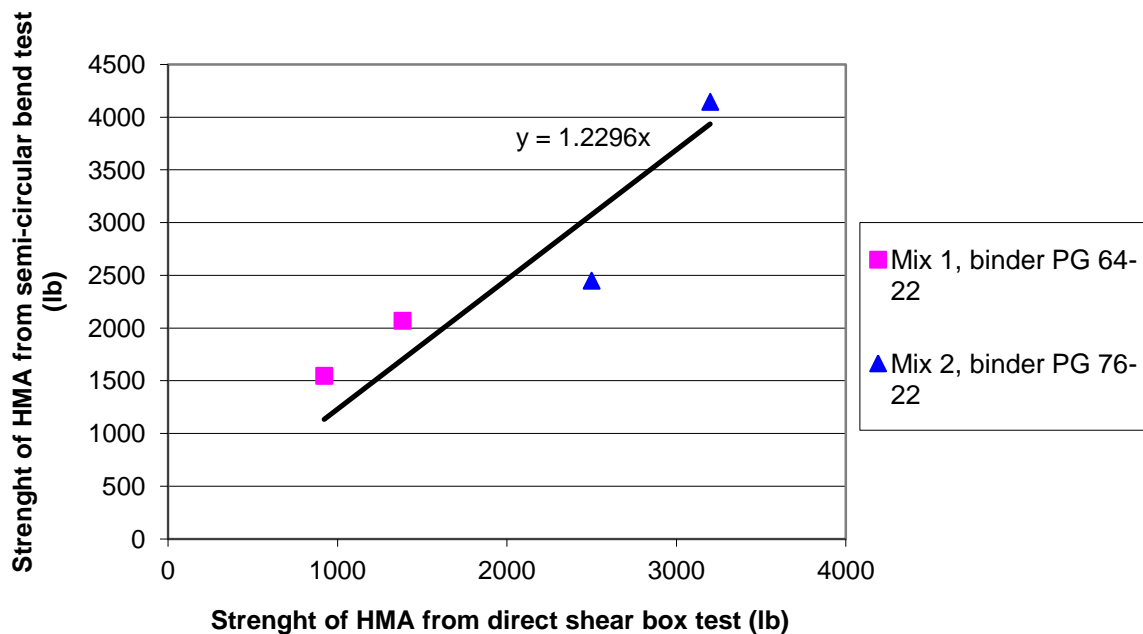
FIGURE 4.39
Correlation of the Peak Loads from the Static Semi-Circular Bend Test and the Direct Shear Box Test with a Gap Width of 0.25 Inch

4.3.2 Direct Shear Test versus Overlay Loading Test

Figure 4.40 shows the comparison of the permanent vertical displacement at the initial crack from the overlay test and the shear displacement from the direct shear box test for both the 1.5 and 2.0 inch thick HMA samples. The comparison shows similar magnitudes of displacements from these two tests and implies that the two displacements are correlated.

4.3.3 Semi-Circular Bend Test versus Overlay Loading Test

Figure 4.41 shows the comparison of the measured tensile strains at the bottom of the specimens at the initial crack from the semi-circular bend test and the overlay test. Since the static load capacity of the 1.5 inch HMA overlay was not measured, it was estimated based on the proportion to the thickness of the specimens as compared with the 2.0 inch HMA overlay (i.e., 1.5/2.0 x 3,000 = 2,250 lbs). It is shown that the semi-circular bend test generally resulted in higher tensile strains than the overlay test because the span between two supports in the semi-

89

circular bend test was 4.8 inches, which was much larger than the gap used in the overlay test. At the larger percent of static load capacity, the cyclic semi-circular bend tests and the overlay tests resulted in closer tensile strains. Even though there is some variability in the HMA overlay (Mix 1) test results, the onset of cracking happened when the tensile strain was greater than 1.0% (only one at 0.6% and one slightly lower than 1.0%). However, Figure 4.29 shows that the Mix 2 specimens had the minimum tolerable tensile strain of 0.6%. Therefore, if the tensile strain in the HMA overlay for both mixes was limited to less than 0.6%, the cracking could be avoided.
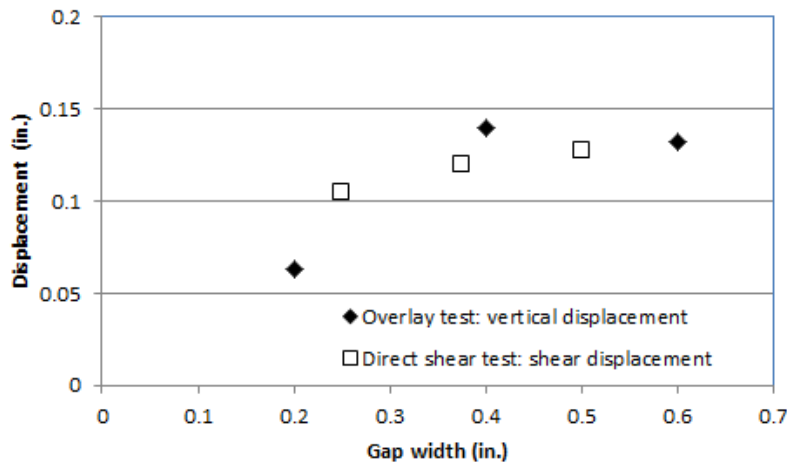
(a) 1.5 inch thick HMA specimens
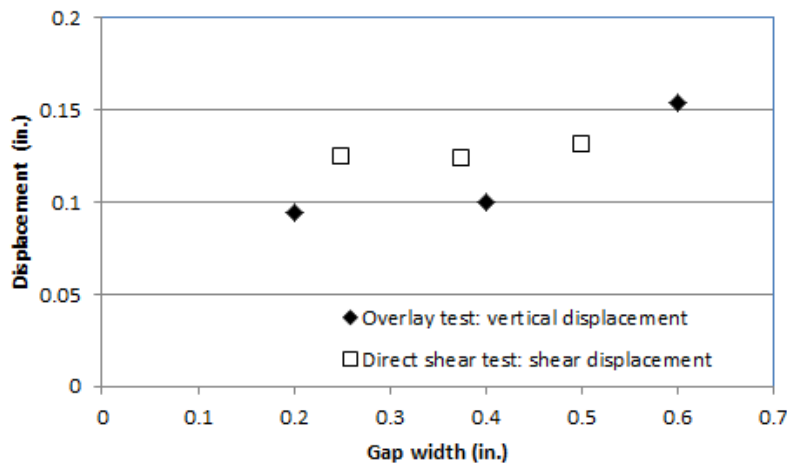
(b) 2.0 inch thick HMA specimens

FIGURE 4.40
Comparison of the Permanent Vertical Displacement at the Initial Crack from the HMA Overlay Test and the Shear Displacement from the Direct Shear Box Test
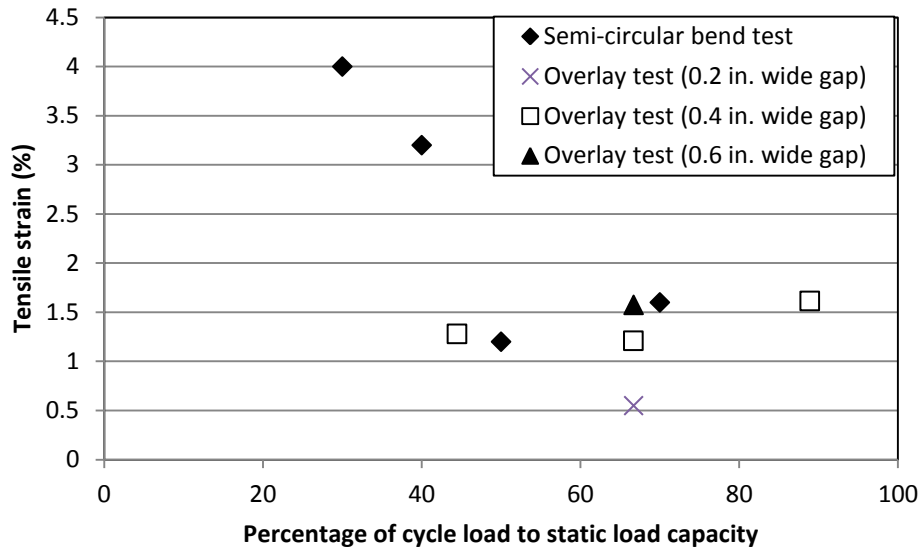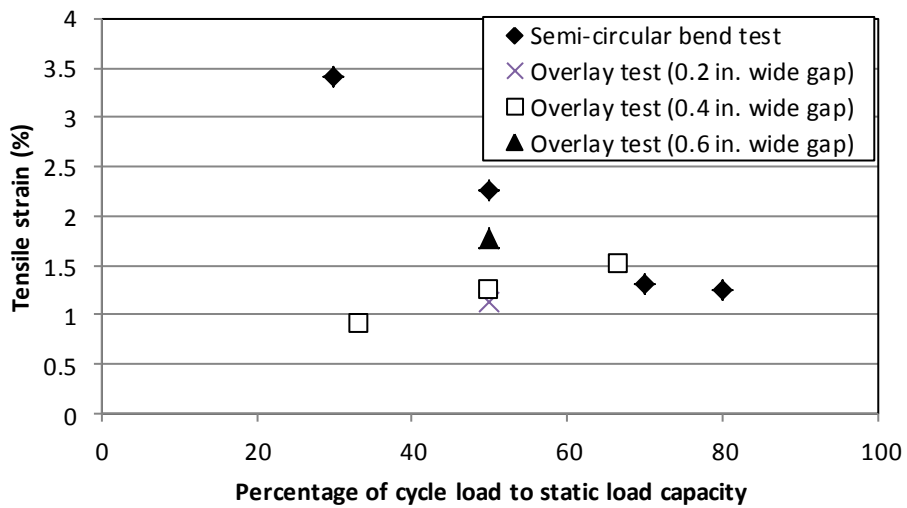
(a) 1.5 inch thick HMA specimens

(b) 2.0 inch thick HMA specimens

FIGURE 4.41
Comparison of the Tensile Strains at the Initial Crack from the Semi-Circular Bend Test and the HMA Overlay Test

Chapter 5: Summary and Conclusions

A laboratory study was conducted to evaluate the shear and tensile characteristics of HMA mixtures chosen from KDOT projects; namely, 089 C-4318-01 (Mix 1) and 56-29 KA-1087-01 (Mix 2). The shear characteristics were obtained by direct shear box tests while the tensile characteristics were obtained by semi-circular bend tests. Fatigue characteristics were obtained by cyclic semi-circular bend tests. The tolerable strains HMA samples can endure were measured by strain gauges in cyclic semi-circular bend tests. The HMA overlay loading tests were performed to verify and correlate the shear and tensile characteristics of HMA mixtures to the performance of the HMA overlays over concrete blocks with different gap thicknesses. All the tests were performed at the room temperatures. Based on the test results obtained from this study, the following conclusions can be drawn:

- Gap width had a minor effect on the maximum shear load and its corresponding shear displacement of the HMA specimen. The shear displacement corresponding to the maximum shear load varied from 6.0% to 9.0 % of the specimen thickness.

- The Mix 2 specimens had higher maximum shear loads and less shear displacements than the Max 1 specimens due to the use of the stiffer asphalt binder.

- Test results show that the direct shear test is an effective method which can evaluate the maximum shear load and its corresponding shear displacement of an HMA mixture.

- Test results show that the semi-circular bend test is an effective method which can characterize the tolerable tensile strain of an HMA mixture. It is shown that Mix 2 was more brittle than Mix 1. The tolerable tensile strain for Mix 1 was from 1.2% to 4% and that of Mix 2 was from 0.6% to 1.4% based on the semi-circular bend tests. However, the tolerable tensile strain for Mix 1 was from 0.6% to 1.8% based on the overlay loading tests.

- The number of loading cycles required to fail an HMA specimen in the semi-circular bend test or the HMA overlay loading test depended on the percentage of the applied load to the maximum static load capacity. In the overlay loading test,

the number of loading cycles also depended on the width of the gap between concrete blocks.

- The HMA overlay on gapped concrete blocks could fail as a result of shear, bending, or a combination of these two failure modes. The wider gap or lower applied load promoted bending failure.

- The peak compressive load of the HMA from the static semi-circular bend test was approximately 1.23 times its peak shear load.

- Specimens at the onset of cracking in the overlay loading tests had permanent vertical displacements with similar magnitudes as shear displacements corresponding to the shear load capacities in the direct shear tests.

- The tolerable tensile strains of HMA specimens in the overlay tests were smaller than those in the semi-circular bend tests; however, an increase of the applied load or gap width minimized their differences.

Based on the HMA mixes, the specimen thicknesses, the gaps between the concrete blocks, the load levels, and the test temperature used in this research, it can be concluded that: (1) the shear failure could be avoided if the shear deformation of the overlay was less than 6% of the HMA overlay thickness and (2) the cracking could be avoided if the tensile strain in the HMA overlay was less than 0.6%. The methods that will limit or prevent that shear deformation and tensile strain should be sought in a future study.

References

Abd El-Naby, R.M., Abd El-Aleem, A.M., and Saber, S.H. 2002. "Evaluation of the Shear Strength of Asphalt Concrete Mixes: Experimental Onvestigation." *Proceedings of Annual Conference of the Canadian Society for Civil Engineering*. Montreal, QB, Canada, Canadian Society for Civil Engineering, 2773–2781.

Arabani, M. and Ferdowsi, B. 2007. "Laboratory Evaluating and Comparison of Semi-Circular Bend Test Results with Other Common Tests for HMA Mixtures." *Advanced Characterization of Pavement and Soil Engineering Materials*, Loizos, Scarpas, and Al-Qadi (eds.). Taylor & Francis Group London, 151–164.

Birgisson, B., Soranakom, C., Napier, J.A.L., and Roque, R. 2003. "Simulation of Fracture Initiation in Hot-Mix Asphalt Mixtures." *Transportation Research Record* 1849, 183–190.

Brown, S.F., Thom, N.H., and Sanders, P.J. 2002. *Reinforced Asphalt.* Final Report to Tensar International., ABG Ltd., Macafferri Ltd., Scott Wilson Pavement Engineering, Bardon Aggregates, 6D Solutions. School of Engineering, University of Nottingham, Nottingham, UK.

Button, J.W. and Lytton, R.L. 2006. "Guidelines for Using Geosynthetics with Hot Mix Asphalt Overlays to Reduce Reflection Cracking." Transportation Research Board Annual Meeting.

Carpenter, S.H., Ghuzlan, K.A., and Shen, S. 2003. "Fatigue Endurance Limit for Highway and Airport Pavements." *Transportation Research Record* 1832, 131–138.

Castell, M.A., Ingraffea, A.R., and Irwin, L.H. 2000. "Fatigue Crack Growth in Pavements." *Journal of Transportation Engineering* 126 (4): 283–290.

Chen, X., Huang, B., and Xu, Z. 2006. "Uniaxial Penetration Testing for Shear Resistance of Hot-Mix Asphalt Mixtures." *Transportation Research Record* 1970, 116–125.

Christensen, D.W. 2003. *Sensitivity Evaluation of Field Shear Test Using Improved Protocol and Indirect Tension Strength Test*. Prepared for NCHRP, Transportation Research Board.

De Bondt, A.H. 1999. *Anti-Reflective Cracking Design of Reinforced Asphaltic Overlay*. Ph.D. dissertation. Delft University of Technology, Netherlands.

Ellis, S.J., Langdale., P.C., and Cook J. 2002. "Performance of Techniques to Minimize Reflection Cracking and Associated Development in Pavement Investigation for Maintenance of UK Military Airfield." Presented for the 2002 Federal Aviation Administration Airport Technology Transfer Conference.

Francken, L., Vanelstraete, A. and de Bondt, A.H. 1997. "Modelling and Structural Design of Overlay Systems." *RILEM Report 18: Prevention of Reflective Cracking in Pavements*, Vanelstraete, A. and Francken, L. (editors). E & FN Spon, London, 84–103.

Ghuzlan, K.A., and Carpenter, S.H. 2000. "Energy-Derived, Damage-Based Failure Criterion for Fatigue Testing." *Transportation Research Record* 1723, 141–149.

Huffman, J.E. 1978. "Reflection Cracking and Control Methods." *Proceedings of the Twenty-third Annual Conference of Canadian Technical Asphalt Association*, 434–443.

Huang, B., Li, G., and Mohammand, L.N. 2003. "Analytical Modeling and Experimental Study of Tensile Strength of Asphalt Concrete Composite at Low Temperature." *Composite, Part B: Engineering.* Elsevier, 705–714.

Huang, B., Shu, X., and Tang, Y. 2005. "Comparison of Semi-Circular Bending and Indirect Tensile Strength Tests for HMA Mixtures." *Proceedings of GeoFrontiers 2005*, Austin, TX, the United States, Geotechnical Special Publication No. 130. American Society of Civil Engineers, 177–188.

Kim, S.-M., Won, M.C., and McCullough, B.F. 2003. "Mechanistic Modeling of Continuously Reinforced Concrete Pavement." *ACI Structural Journal* 100 (5): 674–682.

Kirschke, K.R., and Velinsky, S.A. 1992. "Histogram-Based Approach for Automated Pavement-Crack Sensing." *Journal of Transportation Engineering* 118 (5): 700–710.

Kohler, E.R., and Roesler, J.R. 2005. "Crack Width Measurements in Continuously Reinforced Concrete Pavements," *Journal of Transportation Engineering* 131 (9): 645–652.

Kohler, E.R. and Roesler, J.R. 2006. "Crack Spacing and Crack Width Investigation from Experimental CRCP Sections." *International Journal of Pavement Engineering* 7 (4): 331–340.

Krans, R.L., Tolman, F., and van de Ven, M.F.C. 1996. "Semi-Circular Bending Test: a Practical Crack Growth Test Using Asphalt Concrete Cores." The Third International RILEM Conference, Reflecting Cracking in Pavements, Spon Press, UK.

Kumara, M.W., Gunaratne, M., Lu, J.J., and Dietrich, B. 2004. "Methodology for Random Surface-Initiated Crack Growth Prediction in Asphalt Pavements." *Journal of Materials in Civil Engineering* 16 (2): 175–185.

Lee, S.W., Bae, J.M., Han, S.H., and Stoffels, S.M. 2007. "Evaluation of Optimum Rubblized Depth to Prevent Reflection Cracks." *Journal of Transportation Engineering*. ASCE, 133 (6): 355–361.

Majidzadeh, K., Kauffmann, E.M., and Saraf, C.L. 1971. "Analysis of Fatigue of Paving Mixtures from the Fracture Mechanics Viewpoint." *ASTM Special Technical Publication* 508: 67–84.

Masad, E., Somadevan, N., Bahia, H.U., and Kose, S. 2001. "Modeling and Experimental Measurements of Strain Distribution in Asphalt Mixes." *Journal of Transportation Engineering* 127 (6): 477–485.

Molenaar, A.A.A. 1993. "Evaluation of Pavement Structure with Emphasis on Reflection Cracking." *Proceedings of 2nd International RILEM Conference on Reflection Cracking*. Laige, Belgium, 21–28.

Molenaar, A. A. A., Scarpas, A., Liu, X., and Erkens, S. M. J. G. 2002. "Semi-Circular Bending Test; Simple but Useful?" *Asphalt Paving Technology* 71. Association of Asphalt Paving Technologist, 794–815.

National Asphalt Pavement Association. 1999. *Guidelines for Use of HMA Overlays to Rehabilitate PCC Pavement*. NAPA Information Series 117.

Roberts F.L., Kandhal P.S., Brown E.R., Lee D.Y., and Kennedy T.W. 1996. "Hot Mix Asphalt Materials, Mixture Design, and Construction." *Lanham, Maryland: NAPA Education Foundation.*

Selezneva, O., Darter, M., Zollinger, D., and Shoukry, S. 2003. "Characterization of Transverse Cracking Spatial Variability: Use of Long-Term Pavement Performance Data for Continuously Reinforced Concrete Pavement Design." *Transportation Research Record* 1849: 147–155.

Sherman, G. 1982. *Minimizing Reflection Cracking of Pavement Overlays*. National Cooperative Highway Research Program, Synthesis of Highway Practice.

Shen, S. and Carpenter, S.H. 2005. "Application of the Dissipated Energy Concept in Fatigue Endurance Limit Testing," *Transportation Research Record* 1929, 165–173.

Song, S.H., Paulino, G.H., and Buttlar, W.G. 2006. "Simulation of Crack Propagation in Asphalt Concrete Using an Intrinsic Cohesive Zone Model." *Journal of Engineering Mechanics* 132 (11): 1215–1223.

Vanelstraete, A. and Francken, L. 1997. *Prevention of Reflective Cracking in Pavements*. E & FN Spon.

Walubita, L.F. 2006. "Application of the Calibrated Mechanistic Approach with Surface Energy (CMSE) Measurements for Fatigue Characterization of Asphalt Mixtures." *Journal of the Association for Asphalt Paving Technology* 75: 457–490.

Wang, H.N., Liu, X.J., and Hao, P.W. 2008. "Evaluating the Shear Resistance of Hot Mix Asphalt by Direct Shear Test." *Journal of Testing and Evaluation* 36 (6): 7.

Wang, L., Hoyos, L.R., Mohammad, L., and Abadie, C. 2005. "Characterization of Asphalt Concrete by Multi-Stage True Triaxial Testing." *Journal of ASTM International* 2 (10): 198–207.

K-TRAN

KANSAS TRANSPORTATION RESEARCH
AND
NEW-DEVELOPMENT PROGRAM

AD ASTRA PER ASPERA
Kansas
Department of Transportation